Check for updates

# Complex Generalized Integral Means Spectrum of Drifted Whole-Plane SLE and LLE

Bertrand Duplantier⬡, Yong Han⬡, Chi Nguyen and Michel Zinsmeister

*Dedicated to the Memory of Krzysztof Gawedzki.*

**Abstract.** We present new exact results for the complex generalized integral means spectrum (in the sense of Duplantier et al. (Commun Math Phys 359(3):823–868, 2018)) for two kinds of whole-plane Loewner evolutions driven by a Lévy process:
  (1) The case of a Lévy process with continuous trajectories, which corresponds to Schramm–Loewner evolution $\mathrm{SLE}_\kappa$ with a *drift* term in the Brownian driving function. There is no known result for its standard integral means spectrum, and we show that a natural path to access it goes through the introduction of the complex generalized integral means spectrum, which is obtained via the so-called Liouville quantum gravity.
  (2) The case of symmetric Lévy processes for which we generalize results by Loutsenko and Yermolayeva (J Phys A Math Theor 47(16):165202, 2014, J Phys A Math Theor 52(43):435202, 2019).

## 1. Introduction

"Il apparut que, entre deux vérités du domaine réel, le chemin le plus facile et le plus court passe bien souvent par le domaine complexe."[It came to appear that, between two truths of the real domain, the easiest and shortest path quite often passes through the complex domain] (Paul Painlevé, 1900) [54].

More than 2 decades ago, Oded Schramm [58] introduced his celebrated theory of random growth processes $SLE_\kappa$. As an example, in the so-called chordal case in the half-plane $\mathbb{H}$, it consists of the one-parameter family of Loewner processes driven on the real line $\partial\mathbb{H}$ by $\sqrt{\kappa}B_t$, where $\kappa$ is a nonnegative number and $B_t$ is standard one-dimensional Brownian motion. This is the unique family of random processes satisfying a certain Markov property with continuous driving function, which is symmetric with respect to the imaginary axis. This theory may be generalized along two directions:

(1) One can drop symmetry with respect to the imaginary axis: one then considers $SLE_\kappa$ with a *drift* term, e.g., the chordal Loewner process driven by a random function of the form

$$\lambda(t) = \sqrt{\kappa}B_t + at,$$

where $B_t$ is as before standard one-dimensional Brownian motion and $a \in \mathbb{R}$.

(2) One can drop the continuity assumption while keeping symmetry: the process so obtained is Loewner evolution driven by a Lévy process, called LLE (for Lévy–Loewner evolution).

Notice that the first class of continuous drifted processes coincides with the whole class of LLE processes with continuous trajectories. For $\kappa = 0$, the Loewner process generated by $\lambda(t) = at$ becomes deterministic. Several deterministic chordal Loewner processes, driven by Lip-1/2 functions, were investigated in [41, 44, 45, 53].

In this paper, we shall consider both extended classes in the *whole-plane* case. In order to understand the multifractal spectra of these processes, such as their integral means spectra (*ims*), and in the spirit of references [15, 18, 36, 46, 48–50], we shall first investigate the cases for which the expected complex moments,

$$\mathbb{E}\left[|f'(z)^p|\left|\left(\frac{z}{f(z)}\right)^q\right|\right], \ p, q \in \mathbb{C},$$

may be computed explicitly, to become part of *integrable probability*. Here $f$ stands for the time 0 whole-plane map from $\mathbb{D}$ to the slit plane in the corresponding Loewner process. Note that *complex* values of $(p, q)$ are considered here in the case of whole-plane SLE with drift. In agreement with the citation by P. Painlevé above, the suggested passage by the complex plane will help us discover the precise form of the associated integral means spectrum in the case of $SLE_\kappa$ with drift, via its complex and generalized versions [15].

In Sect. 2, we shall make use of the so-called *Liouville quantum gravity* and *Coulomb gas* techniques, in the spirit of [13, 17, 26, 28], to (non-rigorously) derive the full complex generalized integral means spectrum $\beta_1(p, q; \kappa, a)$ of whole-plane $SLE_\kappa$ with drift $a$ and for $(p, q) \in \mathbb{C}^2$. Section 3 covers SLE integrable cases, which are rigorously solved on a two-dimensional sub-manifold of $\mathbb{C}^2$ which generalizes the integrable parabolas of [15] and [36], and successfully compared with the previous claims. For the generalized spectrum of LLE processes studied in Sect. 4, we shall concentrate on $(p = 2, q \in \mathbb{R})$ integrable

cases, which can be solved analytically by closing some recursions between Fourier modes, in the spirit of [50].

The remainder of the present introductory section is devoted to providing precise definitions, and as a warm-up, to computing the complex generalized spectrum of the logarithmic spiral, in the first $(p, q) \in \mathbb{C}^2$, $\kappa = 0, a \neq 0$ nontrivial case.

## 1.1. Interior Whole-Plane SLE

SLE is a particular case of a growth process called the Loewner process, of which several variants exist, known as *chordal, radial, dipolar,* or *whole-plane* [6,43]. In this work, we will consider the *interior whole-plane* case, which is determined by a *driving function* $\lambda : [0, +\infty) \to \partial\mathbb{D} := \{z \in \mathbb{C} : |z| = 1\}$ obtained as follows. Let us start by defining $\gamma : [0, +\infty) \to \mathbb{C}$ to be a continuous function such that $\lim_{t \to +\infty} |\gamma(t)| = +\infty$ and $\gamma(t) \neq 0, \forall t \geq 0$. Then, for each $t > 0$, the slit domain $\Omega_t = \mathbb{C} \backslash \gamma([t, \infty))$ is a simply connected domain containing 0. By the Riemann mapping theorem, there exists a unique conformal map $f_t : \mathbb{D} \to \Omega_t$ such that $f_t(0) = 0$ and $f_t'(0) > 0$. By the Caratheodory convergence theorem, $f_t$ converges to $f_0$, the Riemann mapping of $\Omega_0$, as $t \to 0$. We may assume without loss of generality that $f_0'(0) = 1$ and, by re-parametrizing the curve if necessary, choose the normalization $f_t'(0) = e^t$. Loewner's theorem asserts that there exists a continuous function $\lambda$ taking values in the unit circle such that

$$\frac{\partial}{\partial t} f_t(z) = z \frac{\partial}{\partial z} f_t(z) \frac{\lambda(t) + z}{\lambda(t) - z}, \quad \lim_{t \to +\infty} f_t(e^{-t}z) = z, \forall z \in \mathbb{D}. \qquad (1.1)$$

The Loewner method can be reversed: given a continuous function $\lambda : [0, +\infty) \to \partial\mathbb{D}$, the partial differential equation (1.1) has a unique solution $f_t(z)$, which is a conformal map from $\mathbb{D}$ onto a domain $\Omega_t$, and the corresponding family $(\Omega_t)_t$ is increasing in $t$. Nevertheless, the domains $\Omega_t$ need not be slit domains as in the example above.

Whole-plane $\mathrm{SLE}_\kappa$ is the process driven by

$$\lambda(t) = e^{i\sqrt{\kappa}B_t},$$

where $\kappa \in [0, +\infty)$ and $B_t$ is standard one-dimensional Brownian motion. Note that when $\kappa = 0$, $f_t(z) = \frac{e^t z}{(1-z)^2}$ is the solution to (1.1), so that $f_0$ is the Koebe function. Thus, as $\kappa \to 0^+$, whole-plane $\mathrm{SLE}_\kappa$ may be seen as a stochastic perturbation of the Koebe map.

In this work, we generalize SLE by adding a drift term to Brownian motion, with a driving function defined as

$$\lambda(t) := e^{i(\sqrt{\kappa}B_t + at)}, a \in \mathbb{R}. \qquad (1.2)$$

The process driven by $\lambda(t)$ then appears for small $\kappa$ as a stochastic perturbation of the ($\kappa = 0$, $a \neq 0$) case of the *logarithmic spiral*.

## 1.2. Complex Generalized Integral Means Spectrum

Let $f$ be a conformal map from $\mathbb{D}$ to $\mathbb{C}$ with $f(0) = 0, f'(0) = 1$. The generalized integral means spectrum of $f$ was originally defined in [15] as follows: for any pair of real numbers $(p, q)$, define the integral moments, for $r \in [0, 1)$,

$$M_f(p, q) := \int_0^{2\pi} r^q \frac{|f'(re^{i\theta})|^p}{|f(re^{i\theta})|^q} \mathrm{d}\theta, \ r \in [0, 1). \tag{1.3}$$

The *generalized integral means spectrum is then defined as*

$$\beta_f(p, q) := \limsup_{r \to 1^-} \left[ \log M_f(p, q) / \log \left( (1-r)^{-1} \right) \right].$$

*If the limit exists, then*

$$M_f(p, q) \dot{\sim} (1-r)^{-\beta_f(p,q)}, \ r \to 1^-, \tag{1.4}$$

*where the notation '$\dot{\sim}$' between two quantities stands for the equivalence of the logarithms of these quantities (i.e., their ratio tends to 1)* [15].

One recovers for $q = 0$ the *standard integral means spectrum*, $\beta_f(p) := \beta_f(p, q = 0)$, which is related by various Legendre transformations to the so-called *multifractal spectra* [30,34,35,38,52], like those governing the moments of the harmonic measure or the continuum of its local singularities [31,51].

For a random simply connected domain as arising from a whole-plane Loewner process with a random driving function like SLE, the question whether the equivalence (1.4) holds *almost surely* is notoriously difficult. Earlier works dealt with the 'expected spectrum' for Brownian motion [25,47], self-avoiding walk [25], percolation [3,24], and SLE [5,9,10,18,26–29,33,55] as well as with the expected generalized spectrum of whole-plane SLE [15]. The almost sure case was solved only recently for the standard spectrum of chordal SLE by Gwynne, Miller and Sun [32] by using the so-called *imaginary geometry* of Miller and Sheffield. (See also the earlier works [40] for the SLE a.s. tip spectrum, [1] for the SLE a.s. boundary spectrum, and the recent work [59] for the $\mathrm{SLE}_\kappa(\rho)$ a.s. boundary spectrum, where imaginary geometry was also used.)

The case of complex moments corresponds to the mixed multifractal spectrum of the harmonic measure and logarithmic rotations of the conformal map [8]. It was studied in expectation in Refs. [7,13,14] for the chordal and radial SLE cases. We shall consider here the whole-plane spectrum defined in expectation for complex moments,

$$\int_{r\partial\mathbb{D}} \mathbb{E}\left[ |f'(z)^p| \left| \left( \frac{z}{f(z)} \right)^q \right| \right] |\mathrm{d}z| \dot{\sim} \left( \frac{1}{1-r} \right)^{\beta(p,q)}, \ p, q \in \mathbb{C}. \tag{1.5}$$

It is then natural to introduce the one-point function

$$G(z) := \mathbb{E}\left[ |f'(z)^p| \left| \left( \frac{z}{f(z)} \right)^q \right| \right], \ p, q \in \mathbb{C}. \tag{1.6}$$

The setting chosen in (1.5) and (1.6) allows for complex values $p, q \in \mathbb{C}$, which we shall need to study the drift case. In the more general case of Lévy processes, we shall see that their defining properties are exactly those needed to obtain

a PDE satisfied by $G$ (1.6), as initiated in Refs. [10,33] and further developed in Refs. [5,15,18] and [46,48–50].

### 1.3. Interior–Exterior Duality

As mentioned in [15], it is interesting to remark that the map $\widehat{f}$,

$$\zeta \in \mathbb{C} \setminus \overline{\mathbb{D}} \mapsto \widehat{f}(\zeta) := 1/f(1/\zeta),$$

is just the *exterior* whole-plane map from $\mathbb{C}\setminus\overline{\mathbb{D}}$ to the slit plane considered in Ref. [10] by Beliaev and Smirnov and in Ref. [5]. We identically have for $0 < r < 1$ and $p \in \mathbb{R}$,

$$\int_{r^{-1}\partial\mathbb{D}} \mathbb{E}\left(|\widehat{f}'(\zeta)|^p\right)|\mathrm{d}\zeta| = r^{2p-2}\int_{r\partial\mathbb{D}} \mathbb{E}\left(\frac{|f'(z)|^p}{|f(z)|^{2p}}\right)|\mathrm{d}z|. \qquad (1.7)$$

We thus see that the standard integral mean of order $(p, q = 0)$ for the exterior whole-plane map studied in [5,10] *coincides* (up to an irrelevant power of $r$) with the $(p, q')$ integral mean for $q' = 2p$, for the interior whole-plane map.

*Remark 1.1. Interior–Exterior Duality.* By conformal inversion, we have for any $p, q \in \mathbb{C}$,

$$\int_{r^{-1}\partial\mathbb{D}} \mathbb{E}\left(\left|\frac{\widehat{f}'(\zeta)^p}{\widehat{f}(\zeta)^q}\right|\right)|\mathrm{d}\zeta| = r^{2\Re p-2}\int_{r\partial\mathbb{D}} \mathbb{E}\left(\left|\frac{f'(z)^p}{f(z)^{2p-q}}\right|\right)|\mathrm{d}z|, \qquad (1.8)$$

so that the $(p, q)$ exterior integral means spectrum coincides with the $(p, q')$ interior integral means spectrum for $q' - p = p - q$. In particular, the $(p \in \mathbb{R}, q' = 0)$ interior derivative moments studied in Ref. [18] correspond to the $(p, q = 2p)$ mixed moments of the exterior map.

### 1.4. Generalized Spectrum for the Logarithmic Spiral

In this section, we give an example of a generalized integral means spectrum, which is deterministic and corresponds to the $\kappa = 0$ case of the drifted $\mathrm{SLE}_\kappa$. It is nothing but the logarithmic spiral with parameter $a \in \mathbb{R}$ (Fig. 1), i.e., the curve parametrized by

$$\gamma(t) = \exp\left[(1 + ia)t\right], \quad t \in \mathbb{R}. \qquad (1.9)$$

**1.4.1. Loewner Process for the Logarithmic Spiral.** Let us define, as before, $\Omega_t := \mathbb{C}\setminus\gamma[t, +\infty)$ and let $f_t : \mathbb{D} \to \Omega_t$ be the associated Riemann map, i.e., the conformal map such that
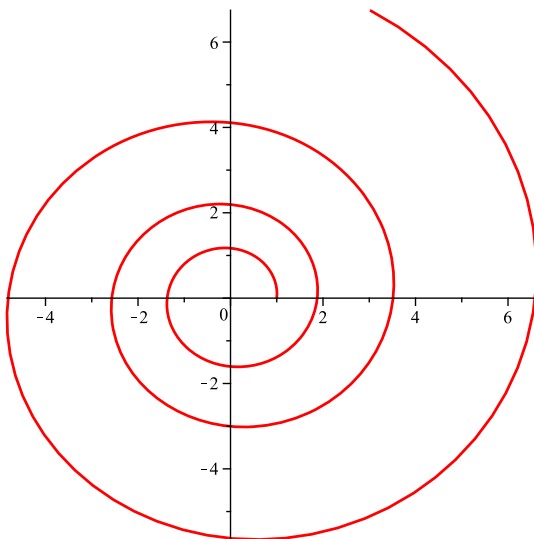
$$f_t(0) = 0, \ f_t'(0) > 0. \qquad (1.10)$$

By the Koebe distortion theorem, $\lim_{t\to-\infty} f_t'(0) = 0$ and $\lim_{t\to+\infty} f_t'(0) = +\infty$. Then, there exists $t_0$ such that $f_{t_0}'(0) = 1$. One also has that $f_{t_0}(e^{i\theta_0}) = \gamma(t_0) = e^{(1+ia)t_0}$ for some $\theta_0 \in [0, 2\pi)$. Consider now the function $\tilde{f}_t$ defined by

$$\tilde{f}_t(z) := e^{(1+ia)t} f_{t_0}(e^{-iat}z).$$

We have $\tilde{f}_t(0) = 0, \tilde{f}_t'(0) = e^t$, and

$$\tilde{f}_t(e^{i(\theta_0+at)}) = e^{(1+ia)(t+t_0)} = \gamma(t + t_0). \qquad (1.11)$$

FIGURE 1. Logarithmic spiral $\gamma(t)$ (1.9) for $a = +5$, restricted to $t \geq 0$

Hence from (1.11), $\tilde{f}_t : \mathbb{D} \to \Omega_{t+t_0}$ is the Loewner process corresponding to the curve

$$\tilde{\gamma}(t) := \gamma(t + t_0), \ t \in \mathbb{R},$$

with the associated driving function $\tilde{\lambda}(t) := e^{i(\theta_0 + at)}$.

Define then the curve,

$$\eta(t) := e^{-i\theta_0}\tilde{\gamma}(t), \ \ t \in \mathbb{R},$$

and the conformal map,

$$h_t(z) := e^{-i\theta_0} \tilde{f}_t(e^{i\theta_0} z).$$

One still has $h_t(0) = 0, h'_t(0) = e^t$, and $h_t(e^{iat}) = \eta(t)$, so that $h_t$ is the Loewner map corresponding to $\eta(t)$ and the associated process is driven by $\lambda(t) := e^{iat}$. Notice that the curve $\eta$ is obtained by a time-translation and a rotation of the logarithmic spiral $\gamma$. Thus, the integral means spectrum will be the same for the time zero Loewner maps $h_0$ and $\tilde{f}_0$.

**1.4.2. Complex Generalized Spectrum for the Complete Logarithmic Spiral.**
We first focus on the *complete* spiral, for which we first establish the following theorem.

**Theorem 1.1.** *The complex generalized integral means spectrum of the complete logarithmic spiral $\gamma(t) = e^{(1+ia)t}$, $t \in \mathbb{R}$, is given, for $p, q \in \mathbb{C}$, by*

$$\beta(p, q; a) = \sup \{0, \beta_1(p, q; 0, a), \beta_2(p, q; 0, a)\}, \tag{1.12}$$

*where*

$$
\begin{aligned}
\beta_1(p, q; 0, a) &:= 2\Re\left(\frac{p - q}{1 - ia}\right) + \Re p - 1, \\
\beta_2(p, q; 0, a) &:= -2\Re\left(\frac{p - q}{1 - ia}\right) + \Re p - 1.
\end{aligned}
\tag{1.13}
$$

*Proof.* Let us define on the unit disk $\mathbb{D}$, the Moebius map $\xi : z \mapsto \xi(z) := i\frac{1-z}{1+z}$, and consider the function $\Phi$ defined on $\mathbb{D}$ as,

$$
\Phi(z) := \exp\left[\frac{2}{1 - ia} \log \xi(z)\right] = \left(i\frac{1 - z}{1 + z}\right)^{\frac{2(1+ia)}{1+a^2}}, \quad z \in \mathbb{D}.
$$

Define also the strip domain $\mathbb{S}_\pi := \{x + iy : x \in \mathbb{R},\ 0 < y < \pi\}$. We know that $z \mapsto \xi(z)$ conformally maps $\mathbb{D}$ onto upper half-plane $\mathbb{H}$, while $z \mapsto \log(z)$ conformally maps $\mathbb{H}$ onto the strip $\mathbb{S}_\pi$. Lastly, $z \mapsto \exp\left(\frac{2}{1-ia} z\right)$ conformally maps the strip domain $\mathbb{S}_\pi$ onto $\mathbb{C} \setminus \gamma$, with a cut along the whole logarithmic spiral $\gamma := \{\gamma(t) = e^{(1+ia)t}, t \in \mathbb{R}\}$. Consequently, $\Phi$ is a conformal map from the unit disk $\mathbb{D}$ to the complement of the *whole* logarithmic spiral $\gamma$, with $\Phi(1) = 0, \Phi(-1) = \infty$.

It enjoys the useful property,

$$
\Phi'(z) = \frac{2}{1 - ia}\left(\log \xi(z)\right)' \Phi(z) = -\frac{4}{1 - ia}\frac{\Phi(z)}{1 - z^2}.
\tag{1.14}
$$

Owing to (1.14), the complex mixed moments of $\Phi$ read

$$
\frac{\Phi'(z)^p}{\Phi(z)^q} = \left(-\frac{4}{1 - ia}\frac{1}{1 - z^2}\right)^p \frac{1}{\Phi(z)^{q-p}},
\tag{1.15}
$$

so that

$$
\left|\frac{\Phi'(z)^p}{\Phi(z)^q}\right| = \left|\left(-\frac{4}{1 - ia}\right)^p\right| \times \frac{|\Phi(z)^{p-q}|}{|(1 - z^2)^p|}.
\tag{1.16}
$$

We have explicitly

$$
\left|(1 - z^2)^p\right| = |1 - z|^{\Re p} |1 + z|^{\Re p} e^{-\Im p \arg(1 - z^2)},
\tag{1.17}
$$

and

$$
\left|\Phi(z)^{p-q}\right| = \exp \Re\left[\frac{2(p - q)}{1 - ia} \log \xi(z)\right].
\tag{1.18}
$$

Setting $b = b(p, q) := \frac{2(p-q)}{1-ia}$, we have $\Re\left[b \log \xi(z)\right] = \Re b \log |\xi(z)| - \Im b \Im \log \xi(z)$, and since $\log \xi(z) \in \mathbb{S}_\pi$, its imaginary part stays *bounded*. We thus have the following (logarithmic) equivalence near the two possible singular points $z = \pm 1$,

$$
\left|\Phi(z)^{p-q}\right| \overset{\cdot}{\sim} |\xi(z)|^{\Re b(p,q)} = \left|\frac{1 - z}{1 + z}\right|^{\Re \frac{2(p-q)}{1-ia}}.
\tag{1.19}
$$

Using (1.16), (1.17), and (1.19), we finally arrive at

$$\left|\frac{\Phi'(z)^p}{\Phi(z)^q}\right| \overset{\cdot}{\sim} \left|\frac{1-z}{1+z}\right|^{\Re\frac{2(p-q)}{1-ia}} |1-z|^{-\Re p} |1+z|^{-\Re p}. \tag{1.20}$$

*Behaviour near infinity and near the origin.* For $z = re^{i\theta}$ near $z = -1$ (point at $\infty$ on the spiral), $|1+z|^2 = r^2 + 2r\cos\theta + 1$ behaves like $(1-r)^2 + (\pi - \theta)^2$. Similarly, near $z = +1$ (point 0 on the spiral), $|1-z|^2$ behaves like $(1-r)^2 + \theta^2$. The integral of (1.20) along the circle $|z| = r$ for $r \to 1^-$ is thus dominated near $z = -1$ by the contribution of the angular neighbourhood of $\theta = \pi$, while near $z = +1$ it is symmetrically dominated by that of the angular neighbourhood of $\theta = 0$. From the explicit form of the integrand (1.20), we readily obtain the overall asymptotic behaviour as $r \to 1^-$ of the integral means,

$$\int_{r\partial\mathbb{D}} \left|\frac{\Phi'(z)^p}{\Phi(z)^q}\right| |\mathrm{d}z| \overset{\cdot}{\sim} (1-r)^{-\beta_\Phi(p,q;a)}, \quad r \to 1^-, \tag{1.21}$$

where the integral means spectrum $\beta_\Phi$ is given by the largest exponent,

$$\beta_\Phi(p,q;a) := \beta_1(p,q;0,a) \vee \beta_2(p,q;0,a) \vee 0, \tag{1.22}$$

with the two dual spectra defined as,

$$\beta_1(p,q;0,a) := 2\Re\frac{p-q}{1-ia} + \Re p - 1, \tag{1.23}$$

$$\beta_2(p,q;0,a) := 2\Re\frac{q-p}{1-ia} + \Re p - 1. \tag{1.24}$$

$\square$

*Remark 1.2. Singularity localization.* Exponent $\beta_1$ is associated with the singularity near $z = -1$ on $\mathbb{D}$ in (1.20), i.e., at *infinity* on the spiral, while $\beta_2$ corresponds to that near $z = +1$, i.e., near the tip at origin 0, around which the spiral *indefinitely winds.*

*Remark 1.3. Conformal invariance by inversion and duality.* The full logarithmic spiral is conformally invariant under the complex inversion, $z \mapsto 1/z$, since $1/\gamma(t) = \gamma(-t)$, and $t \in \mathbb{R}$. This inversion exchanges the roles of origin and infinity and maps the interior of $\mathbb{D}$ to its exterior. The complex generalized integral means spectrum then obeys the *duality property* (1.1). Spectra (1.23) and (1.24) are indeed dual of each other under the corresponding exchange $q - p \mapsto p - q$, resulting in the expected invariance under duality of the integral means spectrum $\beta_\Phi$ (1.22) for the complete logarithmic spiral.

**1.4.3. Complex Generalized Spectrum of the Half Spiral.** Consider now $h_0(z)$, the conformal map corresponding to the whole-plane Loewner process driven by $e^{iat}$, stopped at time $t = 0$, the image of which, $\gamma(t) = e^{(1+ia)t}$, $t \geq 0$, we may call the *half spiral* (Fig. 1). The complex generalized integral means spectrum of the half logarithmic spiral is given by the following theorem. (See Fig. 2.)
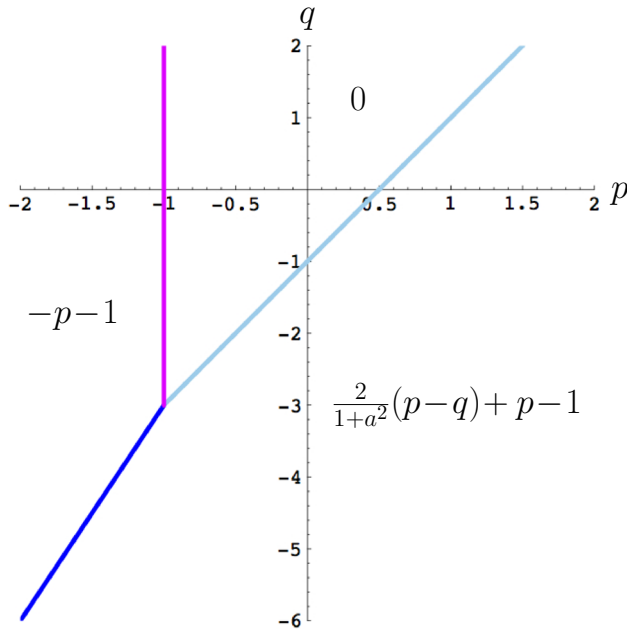
FIGURE 2. The three phases of the generalized integral means spectrum of the logarithmic spiral, with $\beta_{\text{tip}}(p; \kappa = 0) = -p - 1$, $\beta_0(p; \kappa = 0) = 0$, $\beta_1(p, q; \kappa = 0, a) = \frac{2}{1+a^2}(p - q) + p - 1$ (Corollary 1.1)

**Theorem 1.2.** *The complex generalized integral means spectrum of $h_0$, where $h_t$ is the whole-plane Loewner process driven by $\lambda(t) = e^{iat}$, and whose trace is the half logarithmic spiral $\gamma(t) = e^{(1+ia)t}$, $t \geq 0$, is given, for $p, q \in \mathbb{C}$, by*

$$\beta(p, q; \kappa = 0, a) = \sup \left\{ -\Re p - 1, 0, \beta_1(p, q; 0, a) = 2\Re\left(\frac{p - q}{1 - ia}\right) + \Re p - 1 \right\}. \tag{1.25}$$

From this, one immediately deduces the following corollary, which yields the *real* generalized integral means spectrum of the half spiral.

**Corollary 1.1.** *The real generalized integral means spectrum of $h_0$, where $h_t$ is the whole-plane Loewner process driven by $\lambda(t) = e^{iat}$, and whose trace is the half logarithmic spiral $\gamma(t) = e^{(1+ia)t}$, $t \geq 0$, is given, for $p, q \in \mathbb{R}$, by*

$$\beta(p, q; \kappa = 0, a) = \sup \left\{ -p - 1, 0, \beta_1(p, q; 0, a) = 2\frac{p - q}{1 + a^2} + p - 1 \right\}. \tag{1.26}$$

This result for the real case, $p, q \in \mathbb{R}$, is illustrated in Fig. 2.

*Proof.*     • *Behaviour near infinity.* For $t \geq 0$, the half spiral and whole spiral are identical and thus have the same spectrum near infinity. So we use

the conformal map $\Phi$ to calculate the integral means spectrum near $\infty$, i.e., by considering the mixed moments (1.20) for $z \to -1$ only, as well as the corresponding contribution to integral (1.21). Because of Remark 1.2, the associated spectrum is $\beta_1$ (1.23).

- *Behaviour near the tip.* Let $\phi(z) := \frac{z}{(1-z)^2}, z \in \mathbb{D}$, with $\phi(-1) = -\frac{1}{4}, \phi(0) = 0, \phi(1) = \infty$, be the *Koebe function*, conformally mapping the unit disk to the straight cut plane as $\mathbb{D} \mapsto \mathbb{C}\setminus(-\infty, -\frac{1}{4}]$. Let $g$ be the conformal map from $\mathbb{C} \setminus (-\infty, -\frac{1}{4}]$ to the plane cut by the half spiral, $\Omega_0 := \mathbb{C} \setminus \gamma[0, \infty)$, with $g(0) = 0, g(-\frac{1}{4}) = \gamma(0) = 1$. Then $h_0 = g \circ \phi$. Notice that both $g$ and $g'$ are bounded near $\phi(-1) = -\frac{1}{4}$, hence also $h_0$ near $z = -1$. Let us define $r\partial\mathbb{D}_\varepsilon := \{z : |z| = r, |1 + z| < \varepsilon\}$, for some fixed $\varepsilon$ such that $1 - r < \varepsilon < 1$, as the neighbourhood along the circle $r\partial\mathbb{D}$ of the pre-image $z = -1$ by $h_0$ of the half spiral tip $\gamma(0) = 1$. In this domain, we have the logarithmic equivalence, as $r \to 1^-$,

$$\int_{r\partial\mathbb{D}_\varepsilon} \left| \frac{h_0'(z)^p}{h_0(z)^q} \right| |\mathrm{d}z| \ \dot\sim \int_{r\partial\mathbb{D}_\varepsilon} |\phi'(z)^p||\mathrm{d}z|, \ \ r \to 1^-.$$

We thus obtain that the integral means spectrum near the tip of the half spiral is the same as the *ims* near the tip of the half line, which is simply,

$$\beta_{\mathrm{tip}}(p; \kappa = 0) := -\Re p - 1. \tag{1.27}$$

- *Bulk behaviour.* Away from $\infty$ and the tip, the half spiral is rectifiable, and its bulk integral means spectrum is trivial, $\beta_0(p; \kappa = 0) = 0$. This ends the proof of Theorem 1.2.

$\square$

## 2. Complex Generalized Spectrum of Drifted Whole-Plane SLE

### 2.1. Introduction

In this section, we will predict the exact form of the generalized integral means spectrum $\beta_1(p, q; \kappa, a)$ associated with the whole-plane $\mathrm{SLE}_\kappa$ with drift $a$. As we shall see, its most symmetric and simplest form is obtained for the complex generalized spectrum where the exponents are complex variables $p, q \in \mathbb{C}$. We shall use a non-fully rigorous method inherited from theoretical physics. More specifically, we use two-dimensional quantum gravity where the Euclidean Lebesgue measure is replaced by the Liouville quantum measure. This allows us to compute multifractal exponents in Liouville quantum gravity (LQG) for $p \in \mathbb{C}$ in the $q = 0$ case and for any $a \in \mathbb{R}$. The conversion to the complex multifractal spectrum in the Euclidean plane is then obtained by using the celebrated Knizhnik–Polyakov–Zamolodchikov (KPZ) relation [12,16,17,20–22,42,57]. The final step to get the complex generalized spectrum for $q \neq 0$ is then obtained via the introduction of the *packing spectrum,*

$$s_1(p, q; \kappa, a) := \beta_1(p, q; \kappa, a) - \Re p + 1, \tag{2.1}$$

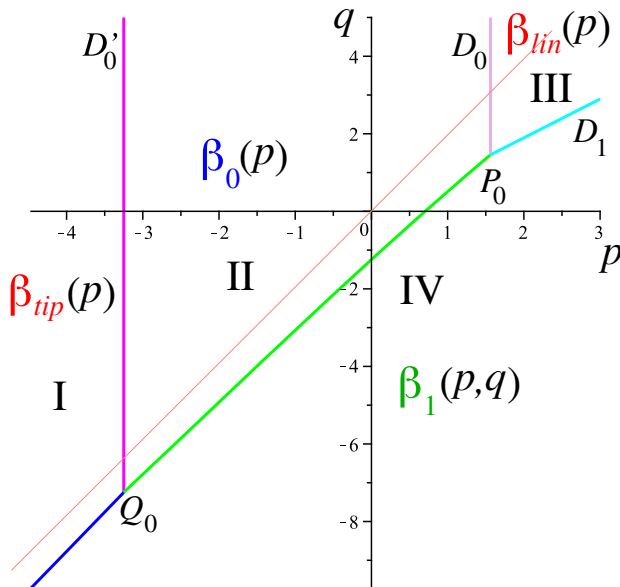*together with the fact that it is a function of variable $p - q$ only.*

FIGURE 3. Phase transition lines for the generalized integral means spectrum of whole-plane SLE$_\kappa$ with no drift $a = 0$. The standard *ims* of the $q = 2p$ exterior version crosses phases I, II, III only, while the $q = 0$ standard *ims* of the interior version crosses phases I, II, IV (from Ref. [15])

## 2.2. Driftless and Real Case

Let us denote by $\beta(p, q; \kappa, a)$ the generalized integral means spectrum of the whole-plane SLE$_\kappa$ with drift coefficient $a$. Ref. [15] studied the $a = 0$ case and for $(p, q) \in \mathbb{R}^2$, for which it is shown that $\beta(p, q; \kappa, a = 0)$ has four possible forms, of which three are independent of $q$,

$$\beta_{\text{tip}}(p; \kappa) := -p - 1 + \frac{1}{4}\left(4 + \kappa - \sqrt{(4 + \kappa)^2 - 8\kappa p}\right), \qquad (2.2)$$

$$\beta_0(p; \kappa) := -p + \frac{4 + \kappa}{4\kappa}\left(4 + \kappa - \sqrt{(4 + \kappa)^2 - 8\kappa p}\right), \qquad (2.3)$$

$$\beta_{\text{lin}}(p; \kappa) := p - \frac{(4 + \kappa)^2}{16\kappa}, \qquad (2.4)$$

$$\beta_1(p, q; \kappa, a = 0) := p + 2(p - q) - \frac{1}{2} - \frac{1}{2}\sqrt{1 + 2\kappa(p - q)}. \qquad (2.5)$$

The separatrices between the different phases are located as follows [15, Theorem 1.7] (see Fig. 3). For $p \leq -1 - \frac{3\kappa}{8}$, there is a (quartic) curve ending at point $Q_0 : p'_0 = -1 - \frac{3\kappa}{8}, q'_0 = -2 - \frac{7\kappa}{8}$, that separates the half-plane into two parts, $\beta$ being equal to $\beta_{\text{tip}}$ above that curve and to $\beta_1$ below it. In the strip $-1 - \frac{3\kappa}{8} \leq p \leq \frac{3(4+\kappa)^2}{32\kappa}$, there is a section of parabola joining $Q_0$ to point
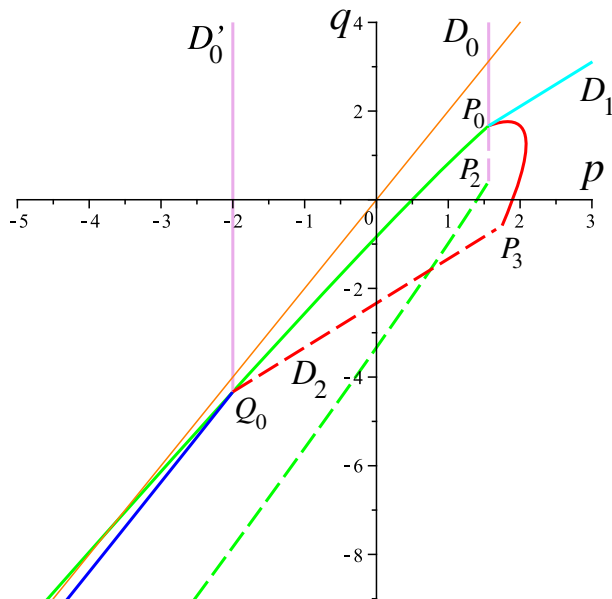
FIGURE 4. Domains of validity of the proofs in the driftless case $a = 0$, $\kappa = 8/3$ (from Ref. [15])

$P_0 = (p_0, q_0)$, with

$$p_0 = \frac{3(4 + \kappa)^2}{32\kappa}, \quad q_0 = \frac{(4 + \kappa)(8 + \kappa)}{16\kappa}, \tag{2.6}$$

that separates the strip into two parts, an upper one where $\beta = \beta_0$ and a lower one where $\beta = \beta_1$. Finally, the half-plane $p \geq p_0$ is similarly split by the half-line with unit slope starting at $P_0$ into an upper part where $\beta = \beta_{\text{lin}}$, while $\beta = \beta_1$ in the lower part. It should be noticed that the generalized spectrum $\beta$ is not everywhere the maximum of the four spectra listed above [15].

The existence of these phase transition lines was established in [15] within a connected semi-infinite domain of the $(p, q)$ plane, as indicated in Fig. 4. This domain of validity sweeps the plane from its upper-left part up to a piecewise boundary first made, for increasing values of $p$, of the dotted green parabola up to its intersection with the straight line $D_2$ of equation $p - q = 1 + \frac{\kappa}{2}$. It then follows this line up to its intersection $P_3 = \left(1 + \frac{2}{\kappa}, \frac{4 - \kappa^2}{2\kappa}\right)$ with the red parabola. From there, the boundary is made of the section of red parabola up to point $P_0$ (2.6), followed by the straight line $D_1$ of equation $q - p = \frac{16 - \kappa^2}{32\kappa}$. These restrictions to the domain of proof are due to technicalities involved in the proofs [5,15,18], and the spectrum is supposed to be still given by $\beta_1$ in the whole connected domain located to the right of the piecewise boundary just described. Recent work by Xuan Hieu Ho extends the domain of validity to the whole interior of the red parabola [37]. Let us now turn to the complex

generalized spectrum of whole-plane SLE for $(p, q) \in \mathbb{C}^2$, possibly with a drift term.

### 2.3. Complex Case with Drift

**Claim 2.1.** *For $p, q \in \mathbb{C}$, and $a = 0$, the complex spectrum $\beta_1$ of whole-plane SLE can be obtained by combining Liouville quantum gravity and Coulomb gas methods. It is*

$$\beta_1(p, q; \kappa, a = 0) = s_1(p - q; \kappa, a = 0) + \Re p - 1 \tag{2.7}$$

$$s_1(p - q; \kappa, a = 0) = s_1(\tau) := 2\tau + \frac{1}{2} - \frac{1}{2}\sqrt{1 + 2\kappa\tau}, \tag{2.8}$$

$$1 + 2\kappa\tau := \frac{1}{2}\left\{1 + 2\kappa\Re(p - q) + |1 + 2\kappa(p - q)|\right\}. \tag{2.9}$$

**Claim 2.2.** *For $a \neq 0$, the complex spectrum $\beta_1$ of whole-plane SLE with drift is given by an extension of the above proofs, as*

$$\beta_1(p, q; \kappa, a) = s_1(p - q; \kappa, a) + \Re p - 1 \tag{2.10}$$

$$s_1(p - q; \kappa, a) = s_1(\tau) := 2\tau + \frac{1}{2} - \frac{1}{2}\sqrt{1 + 2\kappa\tau}, \tag{2.11}$$

$$1 + 2\kappa\tau := \frac{1}{2}\left\{\Re\left[(1 + ia)^2 + 2\kappa(p - q)\right] + \left|(1 + ia)^2 + 2\kappa(p - q)\right|\right\}. \tag{2.12}$$

*Remark 2.1.* In the limit $\kappa \to 0$, the integral means spectrum (1.23) of the half-spiral is recovered from (2.10) (2.11), by observing that the expansion to order $O(\kappa)$ of the r.h.s. of (2.12) indeed yields $\tau = \Re\left(\frac{p-q}{1-ia}\right)$.

As we shall see in Sect. 3.4, this complex spectrum yields the correct answer along an *integrable* complex parabola in the complex space $(p, q) \in \mathbb{C}^2$.

In the *real* moment case, $(p, q) \in \mathbb{R}^2$, the generalized integral means spectrum $\beta_1(p, q; \kappa, a)$ associated with whole-plane $\mathrm{SLE}_\kappa$ with drift $a$ is given by the explicit formulae:

$$\beta_1(p, q; \kappa, a) = p + 2\tau - \frac{1}{2} - \frac{1}{2}\sqrt{1 + 2\kappa\tau}, \tag{2.13}$$

$$1 + 2\kappa\tau := \frac{1}{2}\left\{1 - a^2 + 2\kappa(p - q) + \sqrt{[1 - a^2 + 2\kappa(p - q)]^2 + 4a^2}\right\}. \tag{2.14}$$

**Consequence 2.1.** *Equation (2.14) can be inverted into:*

$$p - q = \tau\left(1 + \frac{a^2}{1 + 2\kappa\tau}\right). \tag{2.15}$$

*Therefore, the phase transition lines in the $(p, p - q)$ plane for $a \neq 0$ are obtained from those for $a = 0$ by the nonlinear transform,*

$$p \mapsto p,$$

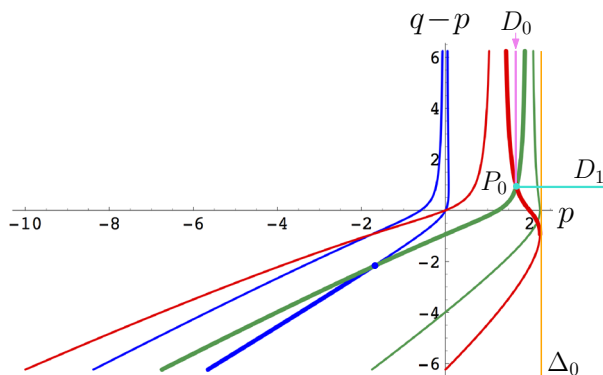$$p - q = \tau \mapsto p - q = \tau\left(1 + \frac{a^2}{1 + 2\kappa\tau}\right). \tag{2.16}$$

FIGURE 5. Nonlinear mapping (2.16) of the red and green parabolas and blue quartic of Ref. [15] (here $\kappa = 2$, $a = 1$)
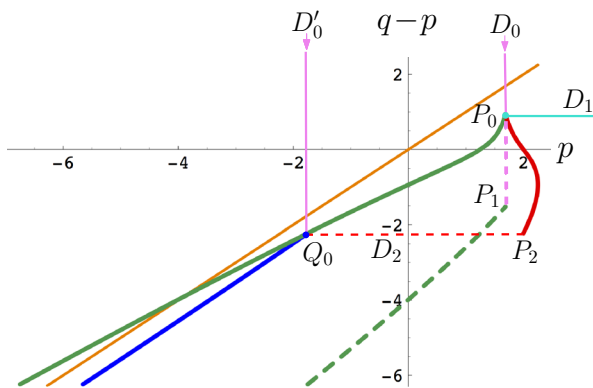


FIGURE 6. Nonlinear mapping (2.16) of the domains of validity of the proofs, as shown in Fig. 4 from [15] (here $\kappa = 2$, $a = 1$)

In the work [15], the location of the various phase transition lines in the case of whole-plane SLE without drift was established with the help of several master curves: a so-called red parabola where the one-point function $G$ (1.6) is integrable, a so-called green parabola where the spectrum changes from $\beta_0$ to $\beta_1$, and a 'blue quartic' where it changes from $\beta_{\text{tip}}$ to $\beta_1$, as well as several straight lines, like $D_0'$ where the spectrum changes from $\beta_{\text{tip}}$ to $\beta_0$, $D_0$ where it changes from $\beta_0$ to $\beta_{\text{lin}}$, and $D_1$ where it changes from $\beta_{\text{lin}}$ to $\beta_1$ (Fig. 3). These curves are also instrumental in delimiting the domains of validity of the proofs (Fig. 4). Applying the nonlinear transform (2.16) in the $(p, q - p)$ plane to these curves yields the corresponding curves in the case of whole-plane SLE with drift. They are illustrated in Figs. 5 and 6.

**2.3.1. Phase Diagram.** Various cases, relative to the values of parameters $\kappa$ and $a$, and drawn thanks to the nonlinear mapping (2.16), are depicted in Figs. 7, 8, 9, and 10. In these figures, it is especially interesting to focus on the standard integral means spectra in the $p, q - p$ plane, obtained for the whole-plane exterior version, along the line $q = 2p$, hence $q - p = p$ (first bisector, golden continuous line), and for the whole-plane interior version along the line $q = 0$, hence $q - p = -p$ (second bisector, golden dotted line).

Point $P_0$ (2.6) in the drift-less case yields a value of $t_0 := p_0 - q_0 = \frac{\kappa^2 - 16}{32\kappa}$, so that $1 + 2\kappa t_0 = \kappa^2/2$. The position of the translated point $P_0 = (p_0, \tilde{q}_0)$ in the presence of drift $a$ is given by Eq. (2.16) as

$$\tilde{q}_0 = p_0 + \frac{16 - \kappa^2}{32\kappa}\left(1 + \frac{16a^2}{\kappa^2}\right). \tag{2.17}$$

To determine whether the first bisector enters region IV as in Fig. 8, so that the *exterior* standard whole-plane spectrum has a $\beta_1$ component, or avoids it as in Fig. 7, we need to know the sign of $\tilde{q}_0 - 2p_0$. If positive, the first bisector passes below $P_0$ so that it successively traverses regions I, II, IV and III as in Fig. 8. Owing to (2.6), this happens for

$$\frac{a^2}{\kappa^2} \geq a_0(\kappa) := \frac{1}{4}\frac{2 + \kappa}{4 - \kappa}, \quad \kappa < 4. \tag{2.18}$$

This phenomenon thus occurs only for simple $SLE_{\kappa<4}$ curves and for a sufficiently strong drift term $a$. Otherwise, one is in the configuration of Figs. 7, 9, and 10 for the first bisector, and the $\beta_1$ spectrum does not appear in the standard *ims* of the exterior whole-plane SLE with drift.

To determine whether the second bisector enters region III and crosses all four phases as in Fig. 10, so that the *interior* standard whole-plane spectrum has a linear component $\beta_{\text{lin}}$, or whether it avoids the linear phase III as in Fig. 9, we need to know the position of $P_0$ with respect to that bisector; hence, the sign of $\tilde{q}_0$. If negative, the second bisector passes above $P_0$, so that it successively traverses regions I, II, III and IV as in Fig. 10. This happens for

$$\frac{a^2}{\kappa^2} \geq \tilde{a}_0(\kappa) := \frac{1}{8}\frac{8 + \kappa}{\kappa - 4}, \quad \kappa > 4. \tag{2.19}$$

This phenomenon thus occurs only for non-simple $SLE_{\kappa>4}$ curves and for a sufficiently strong drift term $a$. Otherwise, one is in the configuration of Figs. 7, 8, and 9 for the second bisector, and the $\beta_{\text{lin}}$ spectrum does not appear in the standard *ims* of the interior whole-plane SLE with drift, which takes the successive forms $\beta_{\text{tip}}, \beta_0, \beta_1$.

*Remark 2.2.* The two conditions on the *reduced drift parameter*, $a/\kappa \geq a_0(\kappa)$, in fact, obey *SLE duality* [23, 26, 28, 29, 61]. Defining the dual SLE parameter $\kappa' = 16/\kappa$, with $\kappa' > 4$ and $\kappa < 4$, one checks that $\tilde{a}_0(\kappa') = \tilde{a}_0(16/\kappa) = a_0(\kappa)$. The occurrence here of this reduced drift parameter $a/\kappa$ may seem natural, if one recalls that the quadratic variation of $\sqrt{\kappa}B_t + at$ is $\kappa t$ and its mean $at$.
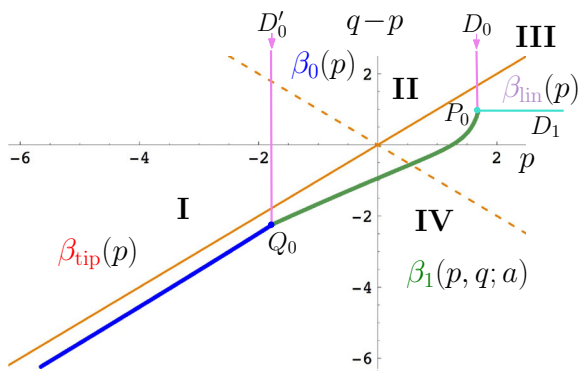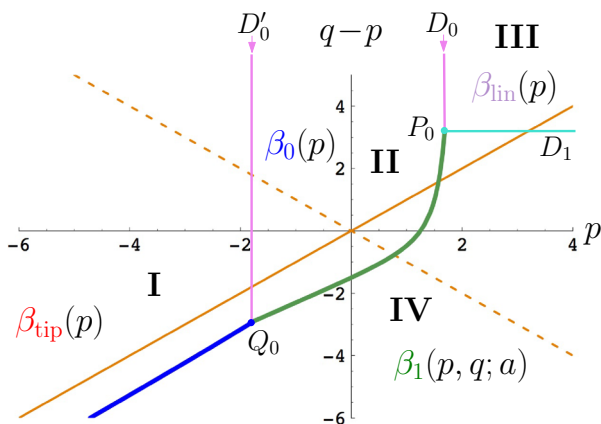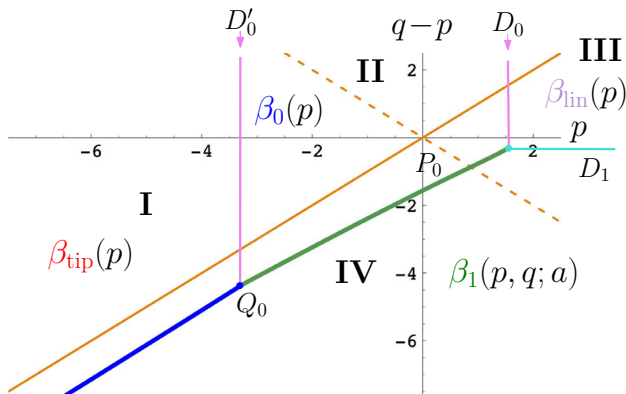
FIGURE 7. Phase transition lines for the generalized integral means spectrum of simple whole-plane $\mathrm{SLE}_\kappa$ with drift (here $\kappa = 2$, $a = 1$). The first bisector with $q = 2p$ (golden continuous line) corresponds to the standard integral means spectrum *(ims)* for the exterior case, which crosses only phases I, II and III, whereas the second bisector with $q = 0$ (golden dotted line) yields the standard *ims* for the interior case, which does enter phase IV with the $\beta_1$ spectrum



FIGURE 8. Phase transition lines for the generalized integral means spectrum of simple whole-plane $\mathrm{SLE}_\kappa$ with drift (here $\kappa = 2$, $a = 2$). The standard *ims* in the $q = 2p$ exterior case crosses all four phases in the order I, II, IV and III, while the $q = 0$ standard *ims* in the interior case crosses phases I, II and IV

FIGURE 9. Phase transition lines for the generalized integral means spectrum of non-simple whole-plane $SLE_\kappa$ with drift (here $\kappa = 6$, $a = 2$). The successive phase crossings of the two standard *ims* bisector lines are analogous to those depicted in Fig. 7
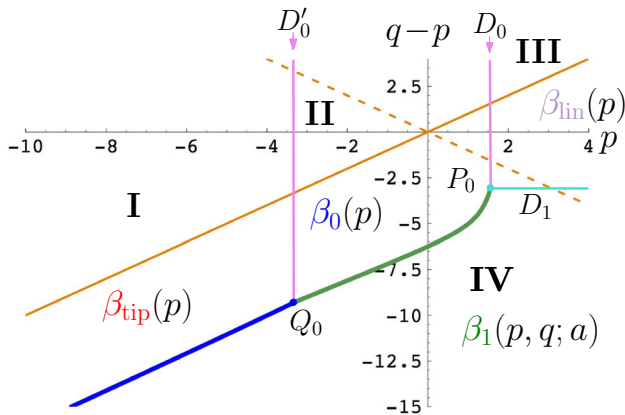


FIGURE 10. Phase transition lines for the generalized integral means spectrum of non-simple whole-plane $SLE_\kappa$ with drift (here $\kappa = 6$, $a = 8$). The standard *ims* in the $q = 2p$ exterior case crosses phases I, II, III only, while the $q = 0$ standard *ims* in the interior case crosses all four phases in the order I, II, III and IV

## 2.4. Derivation of Claims 2.1 and 2.2

**2.4.1. Discourse on the Method.** We are going to use here a *Liouville quantum gravity* (LQG) approach, which historically gave the first derivation of the standard SLE multifractal spectrum [26], which was later confirmed by a standard mathematical approach [5,10,32]. It is based on the celebrated

Knizhnik–Polyakov–Zamolodchikov (KPZ) relation [12, 16, 42] between scaling exponents in the Euclidean plane, and their counterparts under a random LQG measure that gives the scaling limit of the area measure on a random planar map. The KPZ relation is now mathematically proved [19, 21, 57]. Although the LQG method, which originates in theoretical physics, is *heuristic* and not fully rigorous, it often offers the quickest and most natural path to the derivation of scaling exponents and multifractal spectra. It is also intimately related to the recently developed and rigorous *wedge-welding* theory in Liouville quantum gravity [17, 60] (see in particular Appendix B in [17] for a mathematically precise description of the KPZ interpretation.)

**2.4.2. Derivation of Claim 2.1.** Let us first recall that in the original work on whole-plane SLE [18], the novel integral means spectrum, $\beta_1(p; \kappa) := \beta_1(p; q = 0; \kappa, a = 0)$, derived there for $p \in \mathbb{R}$, was related to some Liouville quantum gravity results obtained in [28]. (See [18, Section 1.3].) It was found that the related *packing spectrum*, defined as,

$$s_1(p; \kappa) := \beta_1(p; \kappa) - p + 1, \tag{2.20}$$

is given by

$$s_1(p) = s_1(p; \kappa) := 2p + \frac{1}{2} - \frac{1}{2}\sqrt{1 + 2\kappa p}. \tag{2.21}$$

When seen as a function of $p$, it has for inverse in terms of $s = s_1$,

$$p = \frac{s}{2} + \frac{\kappa}{8}\mathcal{U}_\kappa^{-1}(s),$$

where we defined

$$\mathcal{U}_\kappa^{-1}(x) := \frac{1}{2\kappa}\left(\kappa - 4 + \sqrt{(4-\kappa)^2 + 16\kappa x}\right),$$

$$\mathcal{U}_\kappa(x) := \frac{1}{4}x\left(\kappa x + 4 - \kappa\right),$$

$$\mathcal{V}_\kappa(x) := \mathcal{U}_\kappa\left(\frac{1}{2}\left(x + 1 - \frac{\kappa}{4}\right)\right) = \frac{1}{16\kappa}\left[\kappa^2 x^2 - (4-\kappa)^2\right].$$

Here, $\mathcal{U}_\kappa$ is the KPZ function of Liouville quantum gravity adapted to $\mathrm{SLE}_\kappa$, while $\mathcal{V}_\kappa$ is an associated function that relates boundary scaling dimensions to bulk ones [28, 29]. Here we generalize methods introduced in [13, 26] and expounded in [28, 29], and use notations similar to those of [28], Section 8. For simplicity, we first implicitly assume SLE paths to be simple, i.e., with $\kappa \leq 4$, since the quantum gravity composition rules differ for the simple and non-simple phases of SLE [28, 29]. Nevertheless, the results obtained also hold for $\kappa > 4$. One has the set of identities,

$$p = x_1(s) - x_1, \tag{2.22}$$

$$x_1(s) := 2\mathcal{V}_\kappa\left[\mathcal{U}_\kappa^{-1}(s) + \mathcal{U}_\kappa^{-1}(\tilde{x}_1)\right], \tag{2.23}$$

$$x_1 := x_1(0) = \frac{1}{8\kappa}(6 - \kappa)(2 - \kappa), \tag{2.24}$$

$$\tilde{x}_1 := \frac{6 - \kappa}{2\kappa}, \quad \mathcal{U}_\kappa^{-1}(\tilde{x}_1) = \frac{2}{\kappa}. \tag{2.25}$$

The scaling exponent $x_1(s)$ geometrically corresponds to a configuration where the SLE *tip* is locally avoiding a bunch of $s$ *independent Brownian paths*. The tip here should be understood as the so-called SLE 'second tip' at the origin [5], after inversion of unbounded (interior) whole-plane SLE [18], as in Beliaev and Smirnov's bounded (exterior) version of whole-plane SLE [5, 10].

In the LQG approach, $s$ independent Brownian paths *avoiding* an SLE path near its tip are conformally equivalent to a certain number $k(s)$ of *mutually avoiding* SLEs in a star configuration, given by

$$k(s) = 1 + \frac{\mathcal{U}_\kappa^{-1}(s)}{\mathcal{U}_\kappa^{-1}(\tilde{x}_1)}, \tag{2.26}$$

such that $x_1(s) = 2\mathcal{V}_\kappa(2k(s)/\kappa)$. When $p \in \mathbb{C}$, its imaginary part $\tilde{t} := \Im p$ corresponds to exponentially weighting by $\exp(\tilde{t} \arg \mathcal{C})$ the mutually avoiding SLE-Brownian path configurations $\mathcal{C}$, with local *winding angle* $\arg \mathcal{C}$ around the tip. One can then show by Coulomb gas arguments [13, 14, 28] that the new scaling exponent associated with the tip is

$$\hat{x}_1(s, \tilde{t}) := x_1(s) - \frac{\kappa}{2} \frac{\tilde{t}^2}{k^2(s)}. \tag{2.27}$$

The average logarithmic spiral rotation rate $a$ near the tip is then obtained by Legendre transformation as [13, 28],

$$a = \frac{\partial}{\partial \tilde{t}} \hat{x}_1(s, \tilde{t}). \tag{2.28}$$

On the other hand, the real part of $p$, $t := \Re p$, is now given by the generalization of (2.22),

$$\Re p = t = \hat{x}_1(s, \tilde{t}) - x_1, \tag{2.29}$$

whereas the packing spectrum for complex $p$, $s = s_1(p; \kappa) = \beta_1(p; \kappa) - \Re p + 1$, is still given by (2.21), but now in terms of the reduced variable $\tau$,

$$\tau := x_1(s) - x_1, \tag{2.30}$$

$$s = s_1(\tau) = 2\tau + \frac{1}{2} - \frac{1}{2}\sqrt{1 + 2\kappa\tau}. \tag{2.31}$$

From Eqs. (2.23), (2.26), we find the simple identity [13, 28]

$$\frac{1}{2\kappa} k^2(s) = x_1(s) + b, \quad b = \frac{(4 - \kappa)^2}{8\kappa}. \tag{2.32}$$

We thus find for (2.27) the simple formula,

$$\hat{x}_1(s, \tilde{t}) = x_1(s) - \frac{1}{4} \frac{\tilde{t}^2}{x_1(s) + b}, \tag{2.33}$$

from which (2.29) gives,

$$t = \hat{x}_1(s, \tilde{t}) - x_1 = x_1(s) - x_1 - \frac{1}{4} \frac{\tilde{t}^2}{x_1(s) - x_1 + c}$$

$$= \tau - \frac{1}{4}\frac{\tilde{t}^2}{\tau + c}, \quad c := b + x_1 = \frac{1}{2\kappa}. \tag{2.34}$$

Equation (2.34) is then inverted into

$$\tau = \frac{1}{2}\left(t - c \pm \sqrt{(t+c)^2 + \tilde{t}^2}\right), \tag{2.35}$$

which can be recast as

$$1 + 2\kappa\tau = \frac{1}{2}(1 + 2\kappa t) \pm \frac{1}{2}\sqrt{(1 + 2\kappa t)^2 + 4\kappa^2\tilde{t}^2}. \tag{2.36}$$

For $\tilde{t} = 0$, we have $\tau = t$, which selects the $(+)$-branch in (2.36), and recalling that $t = \Re p, \tilde{t} = \Im p$, we obtain

$$1 + 2\kappa\tau = \frac{1}{2}(1 + 2\kappa\Re p) + \frac{1}{2}\sqrt{(1 + 2\kappa\Re p)^2 + 4\kappa^2\Im p^2}, \tag{2.37}$$

which is the announced complex formula (2.14) for $p \in \mathbb{C}, q = 0$. When $q \neq 0$, we invoke the general validity of the observation made in Ref. [15] that the generalized packing spectrum, $s_1(p, q; \kappa, a = 0) = \beta_1(p, q; \kappa, a = 0) - \Re p + 1$, solely depends on the reduced variable $p - q$, hence $s_1(p, q; \kappa, 0) = s_1(p - q, 0; \kappa, 0)$.          $\square$

**2.4.3. Derivation of Claim 2.2.** When $a \neq 0$, we modify the above aproach as follows. In the absence of Brownian paths, $s = 0$, (2.33) becomes, since $x_1(0) = x_1$,

$$\hat{x}_1(0, \tilde{t}) = x_1(0) - \frac{1}{4}\frac{\tilde{t}^2}{x_1(0) + b} = x_1 - \frac{\kappa}{2}\tilde{t}^2. \tag{2.38}$$

The spiral rotation rate $a$ then corresponds via (2.28) to a parameter $\tilde{t}_0$ such that,

$$a = -\kappa\tilde{t}_0, \quad \hat{x}_1(0, \tilde{t}_0) = x_1 - \frac{a^2}{2\kappa}. \tag{2.39}$$

Re-centring around the spiralling rate $a$, we define, instead of (2.33),

$$\widehat{x}_1(s, \tilde{t}) := x_1(s) - \frac{1}{4}\frac{(\tilde{t} - \tilde{t}_0)^2}{x_1(s) + b}, \tag{2.40}$$

and substitute to (2.29), (2.34)

$$t = \widehat{x}_1(s, \tilde{t}) - \hat{x}_1(0, \tilde{t}_0) = x_1(s) - x_1 + \frac{a^2}{2\kappa} - \frac{1}{4}\frac{(\tilde{t} - \tilde{t}_0)^2}{x_1(s) - x_1 + c}$$

$$= \tau + \frac{a^2}{2\kappa} - \frac{1}{4}\frac{(\tilde{t} - \tilde{t}_0)^2}{\tau + c}, \quad c = \frac{1}{2\kappa}, \quad \tilde{t}_0 = -\frac{a}{\kappa}. \tag{2.41}$$

Thus, instead of (2.35) we find

$$\tau = \frac{1}{2}\left(t - c - \frac{a^2}{2\kappa} \pm \sqrt{\left(t + c - \frac{a^2}{2\kappa}\right)^2 + (\tilde{t} - \tilde{t}_0)^2}\right). \tag{2.42}$$

By again selecting the $(+)$-branch and recalling that $t = \Re p$, $\tilde{t} = \Im p$, this can finally be written as

$$1 + 2\kappa\tau = \frac{1}{2}(1 - a^2 + 2\kappa t) + \frac{1}{2}\sqrt{(1 - a^2 + 2\kappa t)^2 + 4(a + \kappa\tilde{t})^2},$$

$$= \frac{1}{2}\left\{\Re\left[(1 + ia)^2 + 2\kappa p\right] + \left|(1 + ia)^2 + 2\kappa p\right|\right\}. \tag{2.43}$$

This is the announced result (2.12) for $p \in \mathbb{C}, q = 0$. Again, for $q \neq 0$, we invoke the fact [15] that the generalized packing spectrum, $s_1(p, q; \kappa, a) = \beta_1(p, q; \kappa, a) - \Re p + 1$, solely depends on the reduced variable $p - q$. □

## 3. Integrable Probability for Drifted Whole-Plane SLE

In order to anticipate the next section, let us put the computations in a more general setting.

### 3.1. Some Background on Lévy Processes

**Definition 3.1.** A Lévy process is a stochastic process $(L_t)_{t \geq 0}$ such that

(1) $L_0 = 0$ (a.s);
(2) For any discrete ordered set $\{t_i, i \in I_n := \{0, \cdots, n\}\}$, such that $t_0 = 0$ and $0 \leq t_i < t_{i+1}, \forall i \in I_{n-1}$, the successive increments, $L_{t_{i+1}} - L_{t_i}, i \in I_{n-1}$, are all mutually independent;
(3) For any $0 \leq s \leq t$, $L_t - L_s$ has the same law as $L_{t-s}$.
(4) $L_t$ is continuous in probability, $\lim_{t \to 0} \mathbb{P}(|L_t - L_0| > \varepsilon) = 0, \ \forall \varepsilon > 0$, which rules out fixed discontinuities of the path $t \mapsto L_t$.

Notice that Brownian motion is a special Lévy process, and a general difference with Brownian motion is that *random jumps* are allowed. The characteristic function of a Lévy process $L_t$ has the form

$$\mathbb{E}[e^{i\xi L_t}] = e^{-t\eta(\xi)}, \tag{3.1}$$

where $\eta$, called the **Lévy symbol**, is a continuous complex function of $\xi \in \mathbb{R}$, satisfying $\eta(0) = 0$ and $\eta(-\xi) = \overline{\eta(\xi)}$. If $\eta(-\xi) = \eta(\xi)$, $L_t$ is a **symmetric Lévy process**. For Brownian motion, the Lévy symbol is $\eta(\xi) = \frac{\xi^2}{2}$. More generally, the function

$$\eta(\xi) = \frac{|\xi|^\alpha}{2}, \alpha \in (0, 2],$$

is the Lévy symbol of the so-called $\alpha-$stable process.

### 3.2. Derivation of the PDE

The inner whole-plane Loewner process is defined as the solution of the ODE in $\mathbb{C}$

$$\begin{cases} \partial_t g_t(z) = g_t(z)\frac{g_t(z) + \lambda(t)}{g_t(z) - \lambda(t)}, & t \geq 0, \\ \lim_{t \to +\infty} e^t g_t(z) = z, & \forall z \in \mathbb{C}, \end{cases} \tag{3.2}$$

with driving function $\lambda(t) = e^{iL_t}$ where $L_t$ is real-valued; $g_t$ is a conformal mapping from a simply connected domain $\Omega_t \subset \mathbb{C}$ onto $\mathbb{D}$, where $\Omega_t$ is defined as $\Omega_t := \{z \in \mathbb{C} : \tau_z > t\}$, where

$$\tau_z := \sup \left\{ t \in \mathbb{R} : \inf_{s \leq t} |g_s(z) - \lambda(s)| > 0 \right\}.$$

Its inverse function $f_t := g_t^{-1}$ obeys the PDE (1.1),

$$\begin{cases} \partial_t f_t(z) = z f_t'(z) \frac{\lambda(t)+z}{\lambda(t)-z} \\ \lim_{t \to +\infty} f_t(e^{-t}z) = z, \quad \forall z \in \mathbb{D}, \end{cases} \tag{3.3}$$

where $f_t$ is now a mapping from $\mathbb{D}$ to the domain $\Omega_t = \mathbb{C} \setminus K_t$, where the connected set $K_t$ is the hull of the Loewner process. In this section, we will assume $L_t, t \geq 0$, to be a *Lévy process*. The (complex) average integral means spectrum of the conformal map $f = f_0$, where $f_t$ is defined by (3.3), describes the singular behavior of the expectation,

$$\mathbb{E}[|f'(z)^p|] = \mathbb{E}\left[ f'(z)^{\frac{p}{2}} \overline{f'(z)}^{\frac{\bar{p}}{2}} \right], \quad p \in \mathbb{C}. \tag{3.4}$$

Similarly to the method used in [15], we shall consider the Lévy–Loewner evolution (LLE) *two-point function* for $z_1, z_2 \in \mathbb{D}$, defined as,

$$G(z_1, \bar{z}_2) := \mathbb{E}\left[ z_1^{\frac{q}{2}} \frac{f'(z_1)^{\frac{p}{2}}}{f(z_1)^{\frac{q}{2}}} \bar{z}_2^{\frac{\bar{q}}{2}} \frac{\overline{f'(z_2)}^{\frac{\bar{p}}{2}}}{\overline{f(z_2)}^{\frac{\bar{q}}{2}}} \right], \quad p, q \in \mathbb{C}. \tag{3.5}$$

Moment (3.4) is the value $G(z, \bar{z})$ at coinciding points $z_1 = z_2 = z$, for the case $q = \bar{q} = 0$. Following essentially the same approach as was introduced in [5,10,15,56], we aim at finding a partial differential equation satisfied by $G$.

Since $f_t$ obeys a PDE instead of an ODE, the use of Itô calculus is problematic. A way to overcome this difficulty [10] is to consider the ODE (3.2) for negative times and then compare the *reverse* function $g_{-t}$ to the *inverse* $g_t^{-1}$. The details are as follows.

For any fixed $s \geq 0$, define the auxiliary function $g_t^{(s)}$ such that: $g_t^{(s)}(z) = e^{-t}z$ for $t > s$, while for $t \leq s$, $g_t^{(s)}$ is the solution to the differential equation (3.2) with the initial (continuity) condition $g_s^{(s)}(z) = e^{-s}z$,

$$\begin{cases} \partial_t g_t^{(s)}(z) = g_t^{(s)}(z) \frac{g_t^{(s)}(z)+\lambda(t)}{g_t^{(s)}(z)-\lambda(t)}, \quad t \geq 0, \\ g_s^{(s)}(z) = e^{-s}z. \end{cases} \tag{3.6}$$

The family of conformal maps $(g_t^{(s)}(z))_{t \geq 0}$ is illustrated in Fig. 11.

**Lemma 3.1.** *With $g_t$ and $g_t^{(s)}$ defined as above, we have, for any $t \geq 0$,*

$$\lim_{s \to +\infty} g_t^{(s)}(z) = g_t(z).$$

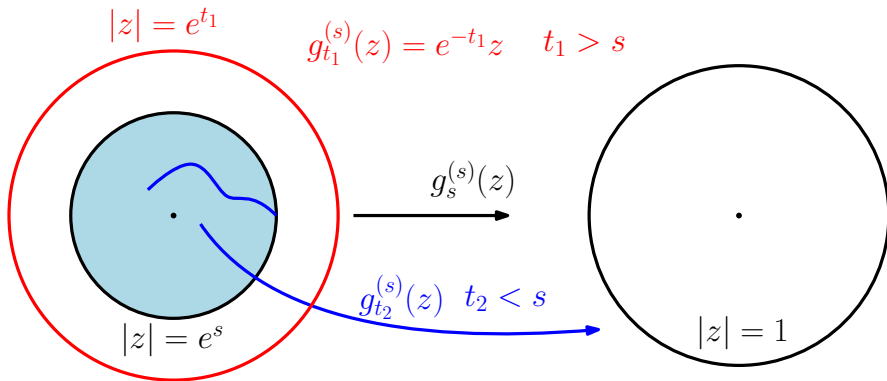This lemma is just the interior version of the following result by Lawler [43] for the exterior whole-plane case.

FIGURE 11. Family of auxiliary conformal maps $(g_t^{(s)})_{t\geq 0}$ for fixed $s \geq 0$. When $0 \leq s \leq t$, $g_t^{(s)}(z) = e^{-t}z$ maps $e^t\mathbb{D}$ onto $\mathbb{D}$, whereas for $0 \leq t \leq s$, $g_t^{(s)}(z)$ maps $e^s\mathbb{D}\backslash K_t$ onto $\mathbb{D}$

**Lemma 3.2** [43, Def. 6.28, Prop. 4.21]. *Let $\tilde{g}_t(z)$ be the solution of the differential equation,*

$$\begin{cases} \partial_t \tilde{g}_t(z) = \tilde{g}_t(z)\frac{\tilde{\lambda}(t)+\tilde{g}_t(z)}{\tilde{\lambda}(t)-\tilde{g}_t(z)}, & t \leq 0, \\ \lim_{t\to-\infty} e^t \tilde{g}_t(z) = z, & \forall z \in \mathbb{C}\backslash\{0\}. \end{cases} \tag{3.7}$$

*For any fixed $s \geq 0$, define $\tilde{g}_t^{(s)}(z)$ as: $\tilde{g}_t^{(s)}(z) = e^{-t}z$ if $t \leq -s$; for $t \geq -s$, $\tilde{g}_t^{(s)}(z)$ is the solution of the above differential equation with initial value $\tilde{g}_{-s}^{(s)}(z) = e^s z$. Then for $t \leq 0$, $\lim_{s\to+\infty} \tilde{g}_t^{(s)}(z) = \tilde{g}_t(z)$.*

In order to prove that Lemma 3.1 follows from Lemma 3.2, one applies complex inversion and time reversal so as to define for $t \leq 0$, $\tilde{g}_t^{(s)}(z) := 1/g_{-t}^{(s)}(1/z)$ and $\tilde{\lambda}(t) := 1/\lambda(-t)$, where $g_t^{(s)}(z)$ is defined by (3.6). Then $\tilde{g}_t^{(s)}$ is as in Lemma 3.2 and for $s \to +\infty$, it converges to the limit $\tilde{g}_t$ obeying (3.7). It then finally suffices to check that $g_t$, defined for $t \geq 0$ as $g_t(z) := 1/\tilde{g}_{-t}(1/z)$, satisfies (3.2).

We then define a reversed radial LLE, as the solution to the ODE in the unit disk $\mathbb{D}$,

$$\partial_t \tilde{f}_t(z) = \tilde{f}_t(z)\frac{\tilde{f}_t(z) + \lambda(t)}{\tilde{f}_t(z) - \lambda(t)}, \quad \tilde{f}_0(z) = z, \ \forall z \in \mathbb{D}, \ t \geq 0. \tag{3.8}$$

**Lemma 3.3.** *For $f_t$ as defined in (3.3) and $\tilde{f}_t$ as defined in (3.8), we have the equivalence in law,*

$$\lim_{t\to+\infty} e^t \tilde{f}_t(z) \overset{(\text{law})}{=} f_0(z). \tag{3.9}$$

*Proof.* For any fixed $s \geq 0$, let $g_t^{(s)}$ be as above. Then, we have $g_t^{(s)}(z) \overset{(\text{law})}{=} \tilde{f}_t(g_0^{(s)}(z))$, because both obey (3.6), and they coincide at $t = 0$ because of

the initial condition in (3.8). We then have, $e^t \tilde{f}_t(z) \overset{\text{(law)}}{=} e^t g_t^{(s)}((g_0^{(s)})^{-1}(z))$.
Letting $s = t$, we get

$$e^t \tilde{f}_t(z) \overset{\text{(law)}}{=} (g_0^{(t)})^{-1}(z), \tag{3.10}$$

and if we let $t \to +\infty$, by Lemma 3.1 we have $\lim_{t \to +\infty} e^t \tilde{f}_t(z) \overset{\text{(law)}}{=} g_0^{-1}(z) = f_0(z)$. $\qquad\qquad\qquad\qquad\qquad\qquad\qquad\qquad\qquad\qquad\qquad\qquad \square$

Let us define the auxiliary, time-dependent, radial variant of the LLE two-point function $G(z_1, \bar{z}_2)$ (3.5),

$$\widetilde{G}(z_1, \bar{z}_2, t) := \mathbb{E}\left[ z_1^{\frac{q}{2}} \frac{\tilde{f}_t'(z_1)^{\frac{p}{2}}}{\tilde{f}_t(z_1)^{\frac{q}{2}}} \bar{z}_2^{\frac{\bar{q}}{2}} \frac{\overline{\tilde{f}_t'(z_2)}^{\frac{\bar{p}}{2}}}{\overline{\tilde{f}_t(z_2)}^{\frac{\bar{q}}{2}}} \right]$$

$$= \mathbb{E}\left[ z_1^{\frac{q}{2}} X_t(z_1) \bar{z}_2^{\frac{\bar{q}}{2}} Y_t(\bar{z}_2) \right], \tag{3.11}$$

where $\tilde{f}_t$ is the reversed radial Loewner process (3.8), together with the shorthand notations,

$$X_t(z) := \frac{\tilde{f}_t'(z)^{\frac{p}{2}}}{\tilde{f}_t(z)^{\frac{q}{2}}}, \quad Y_t(\bar{z}) := \overline{X_t(z)} = \frac{\overline{\tilde{f}_t'(z)}^{\frac{\bar{p}}{2}}}{\overline{\tilde{f}_t(z)}^{\frac{\bar{q}}{2}}}.$$

By using (3.10), where the r.h.s. and its derivative are locally uniformly bounded by the Koebe distortion theorem, the two-point function $G(z_1, \bar{z}_2)$ (3.5) is, by Lebesgue's dominated convergence theorem, the limit

$$\lim_{t \to +\infty} e^{\Re(p-q)t} \widetilde{G}(z_1, \bar{z}_2, t) = G(z_1, \bar{z}_2). \tag{3.12}$$

*Remark 3.1.* The same argument implies that $\widetilde{G}(z_1, \bar{z}_2, t)$ and $G(z_1, \bar{z}_2)$ are holomorphic with respect to both $z_1$ and $\bar{z}_2$.

As explained in [10,56], the idea is then to construct a martingale $\mathcal{M}_s$ related to $\widetilde{G}$. The vanishing of the drift term in its Itô derivative then yields a partial differential equation obeyed by $\widetilde{G}$.

For $s \le t$, define the two-point martingale $(\mathcal{M}_s)_{t \ge s \ge 0}$ with

$$\mathcal{M}_s := \mathbb{E}[X_t(z_1) Y_t(\bar{z}_2) | \mathcal{F}_s],$$

where the random variable is integrable for fixed $z_1$ and $z_2$, and where $\mathcal{F}_s$ is the $\sigma$-algebra generated by the Lévy process filtration $\{L_u, u \le s\}$. By the Markov property of the Lévy process, we know that for any $s \le t$,

$$\tilde{f}_t(z) \overset{\text{(law)}}{=} \lambda(s) \tilde{f}_{t-s}(\tilde{f}_s(z)/\lambda(s)). \tag{3.13}$$

Therefore,

$$\mathcal{M}_s = X_s(z_1) Y_s(\bar{z}_2) \widetilde{G}(z_{1,s}, \bar{z}_{2,s}, \tau), \quad \tau := t - s, \forall \tau > 0, \tag{3.14}$$

where

$$z_{1,s} := \frac{\tilde{f}_s(z_1)}{\lambda(s)}, \quad \bar{z}_{2,s} := \overline{\left( \frac{\tilde{f}_s(z_2)}{\lambda(s)} \right)} = \overline{\tilde{f}_s(z_2)} \lambda(s).$$

In order to prepare for Itô calculus, we have [15, Section 4, Eqs. (47–49)]

$$\mathrm{d}X_s(z_1) = X_s(z_1)\left[\frac{p}{2} - \frac{q}{2} - \frac{p}{(1-z_{1,s})^2} + \frac{q}{1-z_{1,s}}\right]\mathrm{d}s, \qquad (3.15)$$

$$\mathrm{d}Y_s(\bar{z}_2) = Y_s(\bar{z}_2)\left[\frac{\bar{p}}{2} - \frac{\bar{q}}{2} - \frac{\bar{p}}{(1-\bar{z}_{2,s})^2} + \frac{\bar{q}}{1-\bar{z}_{2,s}}\right]\mathrm{d}s, \qquad (3.16)$$

$$\frac{\partial z_{1,s}}{\partial s}\Big|_{\lambda(s)} = z_{1s}\frac{z_{1,s}+1}{z_{1,s}-1}, \quad \frac{\partial \bar{z}_{2,s}}{\partial s}\Big|_{\lambda(s)} = \bar{z}_{2,s}\frac{\bar{z}_{2,s}+1}{\bar{z}_{2,s}-1}. \qquad (3.17)$$

Let us write $\mathcal{M}_s$ as a formal function of two variables,

$$H(s, L_s) := \mathcal{M}_s = X_s(z_1)Y_s(\bar{z}_2)\widetilde{G}(z_{1,s}, \bar{z}_{2,s}, t-s).$$

It is a (local) martingale for all $s \leq t$; thus, by Itô calculus its total $s$-derivative vanishes,

$$\Lambda H(s, L_s) + \partial_s H(s, L_s) = 0,$$

where $\Lambda$ is the generator of the Lévy process $L_s$.

We have from Eqs. (3.15), (3.16), (3.17),

$$\begin{aligned}
\partial_s H = {} & H\left[\frac{p}{2} - \frac{q}{2} - \frac{p}{(1-z_{1,s})^2} + \frac{q}{1-z_{1,s}}\right] \\
& + H\left[\frac{\bar{p}}{2} - \frac{\bar{q}}{2} - \frac{\bar{p}}{(1-\bar{z}_{2,s})^2} + \frac{\bar{q}}{1-\bar{z}_{2,s}}\right] \\
& - X_s(z_1)Y_s(\bar{z}_2)\partial_\tau\widetilde{G}(z_{1,s}, \bar{z}_{2,s}, t-s) \\
& + X_s(z_1)Y_s(\bar{z}_2)\partial_{z_1}\widetilde{G}(z_{1,s}, \bar{z}_{2,s}, t-s)z_{1s}\frac{z_{1,s}+1}{z_{1,s}-1} \\
& + X_s(z_1)Y_s(\bar{z}_2)\partial_{\bar{z}_2}\widetilde{G}(z_{1,s}, \bar{z}_{2,s}, t-s)\bar{z}_{2,s}\frac{\bar{z}_{2,s}+1}{\bar{z}_{2,s}-1},
\end{aligned}$$

where $\tau := t - s$. Since neither $X_s(z)$ nor its complex conjugate $Y_s(z)$ vanish in $\mathbb{D}$, we deduce that

$$\begin{aligned}
-\Lambda\widetilde{G}(z_{1,s}, \bar{z}_{2,s}, t-s) = {} & \widetilde{G}(z_{1,s}, \bar{z}_{2,s}, t-s)\left[\frac{p}{2} - \frac{q}{2} - \frac{p}{(1-z_{1,s})^2} + \frac{q}{1-z_{1,s}}\right] \\
& + \widetilde{G}(z_{1,s}, \bar{z}_{2,s}, t-s)\left[\frac{\bar{p}}{2} - \frac{\bar{q}}{2} - \frac{\bar{p}}{(1-\bar{z}_{2,s})^2} + \frac{\bar{q}}{1-\bar{z}_{2,s}}\right] \\
& - \partial_\tau\widetilde{G}(z_{1,s}, \bar{z}_{2,s}, t-s) + \partial_{z_1}\widetilde{G}(z_{1,s}, \bar{z}_{2,s}, t-s)z_{1s}\frac{z_{1,s}+1}{z_{1,s}-1} \\
& + \partial_{\bar{z}_2}\widetilde{G}(z_{1,s}, \bar{z}_{2,s}, t-s)\bar{z}_{2,s}\frac{\bar{z}_{2,s}+1}{\bar{z}_{2,s}-1}. \qquad (3.18)
\end{aligned}$$

Notice that by (3.12), it holds that, as $t \to +\infty$,

$$\Re(p-q)\exp\left[\Re(p-q)t\right]\widetilde{G}(z_1, \bar{z}_2, t) + \exp\left[\Re(p-q)t\right]\partial_t\widetilde{G}(z_1, \bar{z}_2, t) \to 0,$$

so that

$$\lim_{t\to+\infty}\exp\left[\Re(p-q)t\right]\partial_t\widetilde{G}(z_1, \bar{z}_2, t) = -\Re(p-q)\,G(z_1, z_2). \qquad (3.19)$$

Multiplying both sides of (3.18) by $\exp\left[\Re(p-q)(t-s)\right]$, and letting $t \to +\infty$, we get

$$
\begin{aligned}
-\Lambda G(z_1, \bar{z}_2) = {} & G(z_1, \bar{z}_2)\left[\frac{p}{2} - \frac{q}{2} - \frac{p}{(1-z_1)^2} + \frac{q}{1-z_1}\right] \\
& + G(z_1, \bar{z}_2)\left[\frac{\bar{p}}{2} - \frac{\bar{q}}{2} - \frac{\bar{p}}{(1-\bar{z}_2)^2} + \frac{\bar{q}}{1-\bar{z}_2}\right] \\
& + \Re(p-q)G(z_1, \bar{z}_2) \\
& + \partial_{z_1} G(z_1, \bar{z}_2) z_1 \frac{z_1+1}{z_1-1} + \partial_{\bar{z}_2} G(z_1, \bar{z}_2) \bar{z}_2 \frac{\bar{z}_2+1}{\bar{z}_2-1}.
\end{aligned} \tag{3.20}
$$

We finally get that $G(z_1, \bar{z}_2)$ satisfies $\mathcal{P}(D)\, G(z_1, \bar{z}_2) = 0$, where

$$
\begin{aligned}
\mathcal{P}(D) := {} & \Lambda + z_1 \frac{z_1+1}{z_1-1}\partial_{z_1} + \bar{z}_2 \frac{\bar{z}_2+1}{\bar{z}_2-1}\partial_{\bar{z}_2} + p - q + \bar{p} - \bar{q} \\
& - \frac{p}{(1-z_1)^2} + \frac{q}{1-z_1} - \frac{\bar{p}}{(1-\bar{z}_2)^2} + \frac{\bar{q}}{1-\bar{z}_2}.
\end{aligned} \tag{3.21}
$$

Recall the definition of $\Lambda$ acting on a $C^\infty(\mathbb{R}^2)$ function $u$,

$$
\Lambda u(x) = \lim_{t \downarrow 0} \frac{1}{t}\left(\mathbb{E}^x[u(L_t)] - u(x)\right).
$$

For $k, l \in \mathbb{Z}$, we have for $z = re^{i\theta}$,

$$
\begin{aligned}
\Lambda(z^k \bar{z}^l) &= r^{k+l}\Lambda(e^{i\theta(k-l)}) = r^{k+l}\lim_{t\downarrow 0}\frac{1}{t}\left(\mathbb{E}^\theta[e^{i(k-l)L_t}] - e^{i(k-l)\theta}\right) \\
&= r^{k+l}\lim_{t\downarrow 0}\frac{1}{t}(e^{-t\eta(k-l)} - 1)\,e^{i(k-l)\theta} = -\eta(k-l)z^k\bar{z}^l,
\end{aligned} \tag{3.22}
$$

where $\eta$ is the Lévy symbol of $L_t$.

### 3.3. Drifted Brownian Motion

In this section, we consider the special Lévy process $L_t = at + \sqrt{\kappa}B_t$, where $a \in \mathbb{R}, \kappa \geq 0$ and $B_t$ is standard one-dimensional Brownian motion. These processes are the most general Lévy processes with a.s. continuous trajectories. By definition of the Lévy symbol

$$
\mathbf{E}[e^{i\xi L_t}] = \mathbf{E}[e^{i\xi(at+\sqrt{\kappa}B_t)}] = e^{ia\xi t - t\frac{\kappa}{2}\xi^2} = e^{-t\eta(\xi)}.
$$

So

$$
\eta(\xi) = \frac{\kappa}{2}\xi^2 - ia\xi.
$$

By (3.22), we have

$$
\Lambda(z^k\bar{z}^l) = -\eta(k-l)z^k\bar{z}^l = \left(-\frac{\kappa}{2}(k-l)^2 + ia(k-l)\right)z^k\bar{z}^l,
$$

so that the Lévy generator in the Brownian drift case is explicitly

$$
\Lambda = -\frac{\kappa}{2}(z\partial_z - \bar{z}\partial_{\bar{z}})^2 + ia(z\partial_z - \bar{z}\partial_{\bar{z}}).
$$

The operator in (3.21) thus becomes

$$\mathcal{P}(D) = -\frac{\kappa}{2}(z_1\partial_{z_1} - \bar{z}_2\partial_{\bar{z}_2})^2 + z_1\left(\frac{z_1+1}{z_1-1} + ia\right)\partial_{z_1}$$

$$+ \bar{z}_2\left(\frac{\bar{z}_2+1}{\bar{z}_2-1} - ia\right)\partial_{\bar{z}_2} + p - q + \bar{p} - \bar{q}$$

$$- \frac{p}{(1-z_1)^2} + \frac{q}{1-z_1} - \frac{\bar{p}}{(1-\bar{z}_2)^2} + \frac{\bar{q}}{1-\bar{z}_2}. \qquad (3.23)$$

**3.3.1. Algebraic Solutions.** We want to find some solutions to the PDE

$$\mathcal{P}(D)G(z_1,\bar{z}_2) = 0, \ \ G(0,0) = 1, \qquad (3.24)$$

and follow the method of Ref. [18], by looking for solutions of the form,

$$G(z_1,\bar{z}_2) = (1-z_1)^\alpha(1-\bar{z}_2)^{\bar{\alpha}}P(z_1\bar{z}_2), \ \ P(0) = 1. \qquad (3.25)$$

The action of the partial differential operator $\mathcal{P}(D)$ (3.23) readily gives

$$\mathcal{P}(D)[(1-z_1)^\alpha(1-\bar{z}_2)^{\bar{\alpha}}P(z_1\bar{z}_2)]$$

$$= z_1\bar{z}_2(1-z_1)^{\alpha-1}(1-\bar{z}_2)^{\bar{\alpha}-1}(\kappa\alpha\bar{\alpha}P(z_1\bar{z}_2) + 2(z_1\bar{z}_2-1)P'(z_1\bar{z}_2))$$

$$+ [\mathcal{P}(\partial)(1-z_1)^\alpha](1-\bar{z}_2)^{\bar{\alpha}}P(z_1\bar{z}_2) + [\mathcal{P}(\bar{\partial})(1-\bar{z}_2)^{\bar{\alpha}}](1-z_1)^\alpha P(z_1\bar{z}_2),$$

where

$$\mathcal{P}(\partial) := -\frac{\kappa}{2}(z_1\partial_{z_1})^2 + \left(\frac{z_1+1}{z_1-1} + ia\right)z_1\partial_{z_1} + p - q + \frac{q}{1-z_1} - \frac{p}{(1-z_1)^2},$$

$$\mathcal{P}(\bar{\partial}) := -\frac{\kappa}{2}(\bar{z}_2\partial_{\bar{z}_2})^2 + \left(\frac{\bar{z}_2+1}{\bar{z}_2-1} - ia\right)\bar{z}_2\partial_{\bar{z}_2} + \bar{p} - \bar{q} + \frac{\bar{q}}{1-\bar{z}_2} - \frac{\bar{p}}{(1-\bar{z}_2)^2}.$$
$$(3.26)$$

Notice that as complex conjugates,

$$\forall z \in \mathbb{D}, \ \ \mathcal{P}(\partial)(1-z)^\alpha = 0 \Leftrightarrow \mathcal{P}(\bar{\partial})(1-\bar{z})^{\bar{\alpha}} = 0.$$

So if we have,

$$\mathcal{P}(\partial)(1-z_1)^\alpha = 0, \qquad (3.27)$$

then equation (3.24) reduces for (3.25) to

$$\kappa\alpha\bar{\alpha}P(z_1\bar{z}_2) + 2(z_1\bar{z}_2-1)P'(z_1\bar{z}_2) = 0, \ \ P(0) = 1$$

$$\Leftrightarrow P(z_1\bar{z}_2) = (1-z_1\bar{z}_2)^{-\frac{\kappa}{2}\alpha\bar{\alpha}}. \qquad (3.28)$$

Let us now look for $\alpha$ such that Eq. (3.27) is satisfied. A direct computation readily gives [18],

$$\mathcal{P}(\partial)(1-z)^\alpha = (1-z)^\alpha A + (1-z)^{\alpha-1}B + (1-z)^{\alpha-2}C,$$

where

$$A := -\frac{\kappa}{2}\alpha^2 + (1+ia)\alpha + p - q, \qquad (3.29)$$

$$B := \kappa\alpha^2 - \left(\frac{\kappa}{2} + 3 - ia\right)\alpha + q, \qquad (3.30)$$

$$C := -\frac{\kappa}{2}\alpha^2 + \left(2 + \frac{\kappa}{2}\right)\alpha - p. \qquad (3.31)$$

Notice that $A + B + C = 0$. For any $\alpha \in \mathbb{C}$, the choice of $p, q$ such that $B = 0$ and $C = 0$, yields a solution to (3.27), hence together with (3.28) a solution (3.25) to (3.24).

We thus get the identity for drifted SLE,

$$G(z_1, \bar{z}_2) = \mathbb{E}\left[z_1^{\frac{q}{2}} \frac{f'(z_1)^{\frac{p}{2}}}{f(z_1)^{\frac{q}{2}}} \bar{z}_2^{\frac{\bar{q}}{2}} \frac{\overline{f'(z_2)}^{\frac{\bar{p}}{2}}}{\overline{f(z_2)}^{\frac{\bar{q}}{2}}}\right] = (1 - z_1)^\alpha (1 - \bar{z}_2)^{\bar{\alpha}} (1 - z_1\bar{z}_2)^{-\frac{\kappa}{2}\alpha\bar{\alpha}},$$

(3.32)

where the quadratic equations $B = 0$, $C = 0$ yield $p$ and $q$ in terms of $\alpha \in \mathbb{C}$ under the parametric form,

$$p = -\frac{\kappa}{2}\alpha^2 + \left(2 + \frac{\kappa}{2}\right)\alpha, \qquad \alpha \in \mathbb{C}, \tag{3.33}$$

$$q = -\kappa\alpha^2 + \left(\frac{\kappa}{2} + 3 - ia\right)\alpha. \tag{3.34}$$

These results generalize those found for real $p, q$ and $a = 0$ in [15]. The complex $p, q$ case, still for $a = 0$, has been thoroughly studied in Ref. [36]. These equations generalize in the complex $p, q$ case; hence, in four-dimensional space, the so-called *red parabola* of the real $(p, q)$-plane described in [15]. By Remark 3.1 and [18, Lemma 3.1], the space of holomorphic solutions in $z_1$, $\bar{z}_2$ to the linear PDE in (3.24) is one-dimensional. As a consequence, we have proven the following

**Theorem 3.1.** *Let* $f(z) = f_0(z)$ *where* $f_t$ *is the drifted whole-plane Loewner process driven by* $\lambda(t) = e^{i(at+\sqrt{\kappa}B_t)}, a \in \mathbb{R}$. *For* $(p, q) \in \mathbb{C}^2$, *let the complex 'red parabola'* $\mathcal{R}$ *be defined as the two-dimensional manifold,*

$$p = -\frac{\kappa}{2}\alpha^2 + \left(2 + \frac{\kappa}{2}\right)\alpha, \qquad q - p = -\frac{\kappa}{2}\alpha^2 + (1 - ia)\alpha, \qquad \alpha \in \mathbb{C}. \tag{3.35}$$

*For* $(p, q) \in \mathcal{R}$, $z_1, z_2 \in \mathbb{D}$, *we identically have*

$$G(z_1, \bar{z}_2) = \mathbb{E}\left[z_1^{\frac{q}{2}} \frac{f'(z_1)^{\frac{p}{2}}}{f(z_1)^{\frac{q}{2}}} \bar{z}_2^{\frac{\bar{q}}{2}} \frac{\overline{f'(z_2)}^{\frac{\bar{p}}{2}}}{\overline{f(z_2)}^{\frac{\bar{q}}{2}}}\right] = (1 - z_1)^\alpha (1 - \bar{z}_2)^{\bar{\alpha}} (1 - z_1\bar{z}_2)^{-\frac{\kappa}{2}\alpha\bar{\alpha}}.$$

*In particular, for* $z_1 = z_2 = z$,

$$G(z, \bar{z}) = \mathbb{E}\left[|z^q| \left|\frac{f'(z)^p}{f(z)^q}\right|\right] = (1 - z)^\alpha (1 - \bar{z})^{\bar{\alpha}} (1 - z\bar{z})^{-\frac{\kappa}{2}\alpha\bar{\alpha}}. \tag{3.36}$$

Hence, in the case of the complex red parabola (3.33), (3.34), we find that the complex generalized *bulk* spectrum is simply given by

$$\beta(p, q; \kappa, a) = \frac{1}{2}\kappa|\alpha|^2. \tag{3.37}$$

*Remark 3.2. Tip spectrum.* When $2\Re\alpha + 1 \leq 0$, the presence in (3.36) of the singular factor $|(1 - z)^\alpha|^2$, besides that of the bulk singular one, brings in an extra singular contribution to the integral means near $z = 1$. This yields the new complex generalized *tip* spectrum [5,10,15] along the red parabola (3.35),

$$\beta(p, q; \kappa, a) = \frac{1}{2}\kappa|\alpha|^2 - 2\Re\alpha - 1, \quad 2\Re\alpha \leq -1. \tag{3.38}$$

Let us now turn to the case of *real* points along the complex red parabola $\mathcal{R}$ (3.35).

**Corollary 3.1.** *Let $f(z) = f_0(z)$ where $f_t$ is the drifted whole-plane Loewner process driven by $\lambda(t) = e^{i(at+\sqrt{\kappa}B_t)}$. If $p, q$ take the following values:*

$$p = p(\kappa, a) = \frac{(4+\kappa)^2}{8\kappa}\left(1 + \frac{4a^2}{(2+\kappa)^2}\right), \quad q = q(\kappa, a) = \frac{4+\kappa}{2\kappa}\left(1 + \frac{4a^2}{(2+\kappa)^2}\right);$$

*then the generalized integral means spectrum $\beta(p, q)$ of $f$ is equal to $p$.*

*Proof.* Let us look for exponents $p, q \in \mathbb{R}$, as parameterized by (3.33) and (3.34), with $\alpha = \alpha_1 + i\alpha_2$ and $\alpha_1, \alpha_2 \in \mathbb{R}$. The condition $\Im p = 0$ gives

$$\alpha_2\left(-\kappa\alpha_1 + 2 + \frac{\kappa}{2}\right) = 0,$$

hence either $\alpha_2 = 0$ or $\alpha_1 = (4+\kappa)/2\kappa$. The condition $\Im q = 0$ yields

$$2\kappa\alpha_1\alpha_2 - \left(\frac{\kappa}{2} + 3\right)\alpha_2 + a\alpha_1 = 0.$$

So if $\alpha_2 = 0$, we have either $\alpha_1 = 0$ or $a = 0$. The first case is trivial, while the second one is the driftless case studied in [15]. So, assuming $a \neq 0$, we obtain

$$\alpha_1 = \frac{4+\kappa}{2\kappa}, \quad \alpha_2 = -\frac{a(4+\kappa)}{\kappa(2+\kappa)},$$

and

$$\alpha = \frac{4+\kappa}{2\kappa}\left(1 - i\frac{2a}{2+\kappa}\right),$$

which in turn gives

$$p = p(\kappa, a) := \frac{(4+\kappa)^2}{8\kappa}\left(1 + \frac{4a^2}{(2+\kappa)^2}\right), \tag{3.39}$$

$$q = q(\kappa, a) := \frac{4+\kappa}{2\kappa}\left(1 + \frac{4a^2}{(2+\kappa)^2}\right). \tag{3.40}$$

Notice the further identity $\frac{\kappa}{2}\alpha\bar{\alpha} = p$. So for these special real values of $p$ and $q$ we have

$$\mathbb{E}\left[|z|^q\frac{|f'(z)|^p}{|f(z)|^q}\right] = \frac{|(1-z)^\alpha|^2}{(1-|z|^2)^{\frac{\kappa|\alpha|^2}{2}}}.$$

Notice also that $\Re\alpha > 0$, so that the singularity at $z = 1$ does not contribute to the circle integral

$$\int_{|z|=r<1}\frac{|(1-z)^\alpha|^2}{(1-|z|^2)^{\frac{\kappa|\alpha|^2}{2}}}|dz| \asymp_{r\to1^-} (1-r)^{-\frac{\kappa|\alpha|^2}{2}}.$$

So in the case (3.39) (3.40) the averaged generalized spectrum is simply $\beta(p, q) = p$. $\square$

### 3.4. Check of Integral Means Spectra on the Integrable Complex 'Red Parabola'

As in [15, Section 5.2.1], we will find that along the 'red parabola' $\mathcal{R}$, a succession of explicit complex integral means spectra reproduces the result $\beta := \kappa|\alpha|^2/2$ of Theorem 3.1. In addition to formulae (2.7), (2.9), (2.10), (2.12) for the complex generalized spectrum $\beta_1$ of (drifted) whole-plane SLE, we shall need the SLE complex *bulk* spectrum $\beta_0(p), p \in \mathbb{C}$, and some extensions of both $\beta_0$ and $\beta_1$ [15, Section 5.1].

**3.4.1. SLE Complex Bulk Spectrum.** The SLE complex bulk spectrum $\beta_0(p)$, $p \in \mathbb{C}$, can be obtained from the results of [13,14], and reads [4],

$$\beta_0(p) = s_0(p) + \Re p - 1, \tag{3.41}$$

$$s_0(p) = s_0(t, \tilde{t}), \ \ t := \Re p, \ \ \tilde{t} := \Im p, \tag{3.42}$$

where the expression for $s_0(t, \tilde{t})$ is

$$s_0(t, \tilde{t}) = 1 + b' - t + \sqrt{(b' - t)^2 + \tilde{t}^2} - (2b')^{\frac{1}{2}} \left[ b' - t + \sqrt{(b' - t)^2 + \tilde{t}^2} \right]^{\frac{1}{2}}, \tag{3.43}$$

$$s_0(t, 0) = 1 + 2(b' - t) - 2\sqrt{b'}\sqrt{b' - t}, \ \ \ b' := \frac{(4 + \kappa)^2}{8\kappa}. \tag{3.44}$$

By introducing the variables,

$$\tau_0 := b' - t, \tag{3.45}$$

$$\bar{\tau} := \frac{1}{2} \left[ b' - t + \sqrt{(b' - t)^2 + \tilde{t}^2} \right] = \frac{1}{2} \left( \tau_0 + \sqrt{\tau_0^2 + \tilde{t}^2} \right), \tag{3.46}$$

the function $s_0(t, \tilde{t})$ (3.43) can then be recast as a function of the *single* variable $\bar{\tau}$, as

$$s_0(t, \tilde{t}) = s(\bar{\tau}) := 1 + 2\bar{\tau} - 2\sqrt{b'}\sqrt{\bar{\tau}},$$
$$s_0(t, 0) = s(\tau_0) = 1 + 2\tau_0 - 2\sqrt{b'}\sqrt{\tau_0}. \tag{3.47}$$

**3.4.2. Extensions of Complex Spectra $\beta_0$ and $\beta_1$.** As in Refs. [15,18], it is natural to define auxiliary *pseudo*-integral means spectra, which help in understanding phase transitions that are mediated by overlaps between various analytic expressions of the spectra. They are obtained by restoring the usual sign indeterminacy in front of square root operations [18, Section 4.2], [15, Section 5.1]. Let us define the auxiliary functions,

$$\beta_0^\pm(p) := s_0^\pm(p) + \Re p - 1, \ \ p \in \mathbb{C}, \tag{3.48}$$

$$s_0^\pm(p) = s_0^\pm(t, \tilde{t}) = s^\pm(\bar{\tau}) := 1 + 2\bar{\tau} \pm 2\sqrt{b'}\sqrt{\bar{\tau}},$$

$$\bar{\tau} = \frac{1}{2} \left( \Re(b' - p) + |b' - p| \right), \ \ \ \ b' = \frac{(4 + \kappa)^2}{8\kappa}$$

$$= \frac{1}{2} \left( b' - t + \sqrt{(b' - t)^2 + \tilde{t}^2} \right), \ t := \Re p, \ \tilde{t} := \Im p, \tag{3.49}$$

such that the complex bulk integral means spectrum (3.41) is given by the $(-)$-branch, $\beta_0 \equiv \beta_0^-$. Similarly, we define

$$\beta_1^\pm(p, q; \kappa, a) := s_1^\pm(p - q; \kappa, a) + \Re p - 1, \quad p, q \in \mathbb{C}, \tag{3.50}$$

$$s_1^\pm(p - q; \kappa, a) = s_1^\pm(\tau) := 2\tau + \frac{1}{2} \mp \frac{1}{2}\sqrt{1 + 2\kappa\tau}, \tag{3.51}$$

$$1 + 2\kappa\tau = \frac{1}{2} \left\{ \Re\left[(1 + ia)^2 + 2\kappa(p - q)\right] + \left|(1 + ia)^2 + 2\kappa(p - q)\right| \right\}, \tag{3.52}$$

such that the complex generalized spectrum (2.10) associated with spiral whole-plane SLE is given by the $(+)$-branch, $\beta_1 \equiv \beta_1^+$.

### 3.4.3. Complex Spectra $\beta_1^\pm$ Along $\mathcal{R}$.

From parameterization (3.35), we first find the identity along the red parabola $\mathcal{R}$,

$$(1 + ia)^2 + 2\kappa(p - q) = (1 + ia - \kappa\alpha)^2.$$

Using the general identity,

$$\frac{1}{2} \left[\Re(z^2) + |z^2|\right] = (\Re z)^2, z \in \mathbb{C}, \tag{3.53}$$

we find for (3.52),

$$1 + 2\kappa\tau = [\Re(1 + ia - \kappa\alpha)]^2 = (1 - \kappa\Re\alpha)^2,$$

so that $s_1^\pm$ (3.51) reads

$$s_1^\pm(\tau) = \frac{1}{\kappa} \left[(1 - \kappa\Re\alpha)^2 - 1\right] + \frac{1}{2} \mp \frac{1}{2}|1 - \kappa\Re\alpha|.$$

We simultaneously have from (3.35) and (3.53),

$$\Re p = -\frac{\kappa}{2}\Re(\alpha^2) + \left(2 + \frac{\kappa}{2}\right)\Re\alpha = \frac{\kappa}{2}|\alpha^2| - \kappa(\Re\alpha)^2 + \left(2 + \frac{\kappa}{2}\right)\Re\alpha. \tag{3.54}$$

Combining the last two equations gives

$$s_1^\pm(\tau) + \Re p - 1 = \frac{\kappa}{2}|\alpha^2| + \frac{\kappa}{2}\Re\alpha - \frac{1}{2} \mp \frac{1}{2}|1 - \kappa\Re\alpha|.$$

Therefore, we get for (3.50) the branch-dependent identity,

$$\beta_1^\pm(p, q; \kappa, a) = s_1^\pm(\tau) + \Re p - 1 = \frac{\kappa}{2}|\alpha^2|, \quad \kappa\Re\alpha \gtreqless 1. \tag{3.55}$$

This shows that the result of Theorem 3.1 for spiral whole-plane SLE is recovered for $\Re\alpha \geq 1/\kappa$ by the 'physical' branch $\beta_1^+$ of the generalized complex spectrum, and for $\Re\alpha \leq 1/\kappa$ by its 'unphysical' branch $\beta_1^-$, in a way entirely similar to the real case studied in [15, Section 5.2.1].

**3.4.4. Complex Spectra $\beta_0^\pm$ Along $\mathcal{R}$.** From parameterization (3.35), we first get the identity,

$$b' - p = \frac{\kappa}{2}\left(\alpha - \frac{4+\kappa}{2\kappa}\right)^2,$$

from which we deduce with the help of (3.53),

$$\bar{\tau} = \frac{1}{2}\big(\Re(b'-p) + |b'-p|\big) = \frac{\kappa}{2}\left(\Re\alpha - \frac{4+\kappa}{2\kappa}\right)^2.$$

This in turn gives

$$s_0^\pm(\bar{\tau}) = 1 + \kappa\left(\Re\alpha - \frac{4+\kappa}{2\kappa}\right)^2 \pm \left(2 + \frac{\kappa}{2}\right)\left|\Re\alpha - \frac{4+\kappa}{2\kappa}\right|,$$

which, together with (3.54) yields

$$s_0^\pm(\bar{\tau}) + \Re p - 1 = \frac{\kappa}{2}|\alpha^2| - \left(2 + \frac{\kappa}{2}\right)\Re\alpha + \kappa\left(\frac{4+\kappa}{2\kappa}\right)^2 \pm \left(2 + \frac{\kappa}{2}\right)\left|\Re\alpha - \frac{4+\kappa}{2\kappa}\right|.$$

Thus, we find the branch-dependent identity,

$$\beta_0^\pm(p;\kappa) = s_0^\pm(\bar{\tau}) + \Re p - 1 = \frac{\kappa}{2}|\alpha^2|, \;\; \kappa\Re\alpha \gtreqless 2 + \frac{\kappa}{2}. \qquad (3.56)$$

We thus see that the result of Theorem 3.1 for spiral whole-plane SLE is recovered for $\Re\alpha \leq 2/\kappa + 1/2$ by the 'physical' branch $\beta_0^-$ of the standard complex spectrum, and for $\Re\alpha \geq 2/\kappa + 1/2$ by its 'unphysical' branch $\beta_0^+$, in a way again similar to the real case studied in [15, Section 5.2.1]. We thus arrive at

**Proposition 3.1.** *Along the red parabola $\mathcal{R}$ (3.35), the integral means spectrum of the drifted whole-plane SLE is successively given by*

$$\beta_0^-(p;\kappa) = \beta_1^-(p,q;\kappa,a) = \frac{\kappa}{2}|\alpha^2|, \;\; \Re\alpha \in (-\infty, 1/\kappa],$$

$$\beta_0^-(p;\kappa) = \beta_1^+(p,q;\kappa,a) = \frac{\kappa}{2}|\alpha^2|, \;\; \Re\alpha \in [1/\kappa, 2/\kappa + 1/2],$$

$$\beta_0^+(p;\kappa) = \beta_1^+(p,q;\kappa,a) = \frac{\kappa}{2}|\alpha^2|, \;\; \Re\alpha \in [2/\kappa + 1/2, +\infty).$$

*Remark 3.3.* The two 'physical' integral means spectra $\beta_0^-$ (3.41) and $\beta_1^+$ (2.10) overlap along the red parabola $\mathcal{R}$ (3.35) in the interval $\Re\alpha \in [1/\kappa, 2/\kappa + 1/2]$, a result which can be directly compared to [15, Eqs. (93)–(95)]. The integral means spectrum is always given by one of those two 'physical' spectra, which coincides with the 'physical' branch of the other spectrum in the preceding overlap interval, or with its 'unphysical' branch outside the said interval.

This corresponds to the presence of a two-dimensional "overlap ribbon" on the red parabola, where the complex generalized integral means spectrum takes both the $\beta_0^-$ and $\beta_1^+$ forms. In the 4-dimensional $(p,q)$ space, there exists a larger *phase-transition* manifold, that is defined by the single condition that these two spectra are equal. This three-dimensional manifold must intersect the above overlap ribbon on a certain phase-transition *line*. The study of such phase-transition manifolds is left to a future work.

## 4. General Lévy Processes with Special Symbols

In this section, we generalize the results in [15, 18, 46, 48, 49] and [50] to the generalized integral means spectrum: in other words, we investigate the values of $(p, q)$ for which the generalized integral means spectrum for Lévy–Loewner evolution has an exact form.

For this purpose, we assume in this section that $G(z, \bar{z})$ (3.5) may be written as

$$G(z, \bar{z}) = (1 - z)(1 - \bar{z})h(z, \bar{z}),$$

where $h(z, \bar{z})$ is *separately analytic* with respect to $z$ and $\bar{z}$ and satisfies the boundary condition $h(0, 0) = 1$. By applying (3.21), we get

$$\Lambda\left[(1 - z)(1 - \bar{z})h\right]$$
$$+ \left[\bar{q}(1 - z) - \bar{p}\frac{1 - z}{1 - \bar{z}} + q(1 - \bar{z}) - p\frac{1 - \bar{z}}{1 - z} + (\bar{p} - \bar{q} + p - q)(1 - z)(1 - \bar{z})\right]h$$
$$+ \frac{1 - z}{1 - \bar{z}}\bar{z}(1 + \bar{z})(h + (\bar{z} - 1)\partial_{\bar{z}}h) + \frac{1 - \bar{z}}{1 - z}z(1 + z)(h + (z - 1)\partial_z h) = 0$$

The coefficient of $h = h(z, \bar{z})$ in this equation is the sum of a polynomial in $z$, $\bar{z}$, and of the polar part,

$$\frac{1 - \bar{z}}{1 - z}\left[-p + z(1 + z)\right] + \frac{1 - z}{1 - \bar{z}}\left[-\bar{p} + \bar{z}(1 + \bar{z})\right].$$

The latter clearly becomes pole-free, i.e., a polynomial in $z$, $\bar{z}$ if and only if $p = \bar{p} = 2$, which we shall hereafter assume. Under this condition, the above equation becomes

$$\Lambda[(1 - z)(1 - \bar{z})h] + (z + 1)(\bar{z} - 1)z\partial_z h + (\bar{z} + 1)(z - 1)\bar{z}\partial_{\bar{z}}h$$
$$+ \left[(z - 1)(3 - \bar{q})\bar{z} + (\bar{z} - 1)(3 - q)z\right]h = 0. \tag{4.1}$$

Besides the restriction to $p = 2$, we shall also assume that $q \in \mathbb{R}$ and that the Lévy process $L_t$ is symmetric. We then get

$$\Lambda[(1 - z)(1 - \bar{z})h] + (z + 1)(\bar{z} - 1)z\partial_z h + (\bar{z} + 1)(z - 1)\bar{z}\partial_{\bar{z}}h$$
$$+ (3 - q)(2z\bar{z} - z - \bar{z})h = 0. \tag{4.2}$$

In order to analyse this equation, we use the Fourier expansion of $t \mapsto h(re^{it}, re^{-it})$:

$$h(z, \bar{z}) = \sum_{n=-\infty}^{+\infty} \theta_n(\xi)z^n, \ \xi := z\bar{z}, \ z = re^{it}. \tag{4.3}$$

When replacing $h$ by this expansion in the equation, we get a recursion formula between the $\theta_n$'s for $n \in \mathbb{Z}$. More precisely, by writing that the $n$'th Fourier coefficient of the left side of (4.2) vanishes, we obtain for $n \in \mathbb{Z}$,

$$2\xi(\xi - 1)\theta_n'(\xi) - \left(\eta_n + n + (\eta_n + 2q - n - 6)\xi\right)\theta_n$$
$$+ \xi\left(\eta_n + n + q - 2\right)\theta_{n+1}(\xi) + (\eta_n - n + q - 2)\theta_{n-1}(\xi) = 0. \tag{4.4}$$

Note that the assumption that $L_t$ is symmetric implies that $h(z, \bar{z})$ is symmetric w.r.t. $z$ and $\bar{z}$, which translates into,

$$\theta_{-n}(\xi) = \xi^n \theta_n(\xi), \tag{4.5}$$

from which we may simply recast expansion (4.3) above as

$$h(z, \bar{z}) = \theta_0(\xi) + \sum_{n=1}^{\infty} \theta_n(\xi)(z^n + \bar{z}^n) = \theta_0(\xi) + \sum_{n=1}^{\infty} 2\theta_n(\xi) r^n \cos nt. \tag{4.6}$$

Before continuing, let us recall that we are looking for the integral means, i.e., the angular integrals,

$$I(r) = \int_0^{2\pi} G(re^{it}, re^{-it}) dt,$$

that can be easily expressed in terms of $\theta_j$'s as

$$\frac{I(r)}{2\pi} = (1 + r^2)\theta_0(r^2) - 2r^2 \theta_1(r^2), \tag{4.7}$$

so that we only need to compute $\theta_0$ and $\theta_1$. For later purposes, let us also mention that $\theta_0(0) = 1$. We thus focus on the equations for $n = 0$ and $n = 1$ (recall that $\eta_0 = 0$ and that $\theta_{-1}(\xi) = \xi \theta_1(\xi)$),

$$(\xi - 1)\theta_0'(\xi) - (q - 3)\theta_0(\xi) + (q - 2)\theta_1(\xi) = 0, \tag{4.8}$$

$$2\xi(\xi - 1)\theta_1'(\xi) - [\eta_1 + 1 + (\eta_1 + 2q - 7)\xi]\,\theta_1(\xi) + (\eta_1 + q - 1)\xi \theta_2(\xi)$$
$$+ (\eta_1 + q - 3)\theta_0(\xi) = 0. \tag{4.9}$$

There are two simple cases where we can explicitly compute $\theta_0$ and $\theta_1$.

(1) The first case is when the coefficient of the $\theta_0$-term in the second equation vanishes, i.e., when

$$\eta_1 = 3 - q, \tag{4.10}$$

which requires $q < 3$. In this case we may take $\theta_1 = 0$ (and actually $\theta_n = 0$ for $n \geq 1$) and $\theta_0$ to be the solution to

$$(\xi - 1)\theta_0'(\xi) - (q - 3)\theta_0(\xi) = 0, \; \theta_0(0) = 1.$$

This gives

$$h(z, \bar{z}) = \theta_0(\xi) = \frac{1}{(1 - \xi)^{3-q}}, \tag{4.11}$$

and

$$G(z, \bar{z}) = \frac{(1 - z)(1 - \bar{z})}{(1 - z\bar{z})^{3-q}},$$

so that $\beta(2, q) = 3 - q > 0$.

(2) The second case is by letting the coefficient of the $\theta_2$-term vanish in the second equation, i.e., by taking

$$\eta_1 = 1 - q, \tag{4.12}$$

which requires $q \leq 1$. We then get a system of coupled ODEs for $\theta_0$ and $\theta_1$, which we must solve with initial data $\theta_0(0) = 1$, $\theta_1(0)$ finite. We find

$$\begin{cases} \theta_0(\xi) = (1 + \xi)(1 - \xi)^{-(4-q)} \\ \theta_1(\xi) = -\frac{2}{2-q}(1 - \xi)^{-(4-q)}, \end{cases} \tag{4.13}$$

from which we deduce that $\beta(2, q) = 4 - q(> 3)$.

Equations (4.11) and (4.13) generalize results of Ref. [49] to $q \neq 0$.

As noticed in [50], the preceding method generalizes: more precisely for any $n \geq 1$, if we let the coefficient of the $\theta_{n-1}$-term vanish in the $n$th equation, i.e., by taking $\eta_n = 2-q+n$, then the solution of the system is $\theta_p = 0$ for $p \geq n$, while $\theta_0, ..., \theta_{n-1}$ are the solutions of the $n$ first equations, with the initial data $\theta_0(0) = 1$. Another possible generalization is by letting vanish, again in the $n$th equation, the coefficient of the $\theta_{n+1}$-term, i.e., by taking $\eta_n = 2 - q - n$; then, the $n$ first equations allow us to compute $\theta_0, ..., \theta_{n-1}$, which is more than needed since we only need to know $\theta_0$ and $\theta_1$. Having dealt in the last section with the $n = 1$ case, let us now investigate the $n = 2$ case.

### 4.1. The $\eta_2 = 4 - q$ Case

We take $\theta_{n \geq 2} = 0$ and have to solve the following system of differential equations:

$$\begin{cases} (x - 1)\theta_0'(x) + (3 - q)\theta_0(x) + (q - 2)\theta_1(x) = 0 \\ 2x(x - 1)\theta_1'(x) - [1 + \eta_1 + (\eta_1 + 2q - 7)x]\,\theta_1(x) + (\eta_1 - 3 + q)\theta_0(x) = 0. \end{cases}$$

We can assume the existence of a real number $\delta$ (to be determined later) and of two functions $f_0, f_1 : [0, 1] \rightarrow \mathbb{R}$ such that $\theta_0$ and $\theta_1$ have the following form,

$$\theta_0(x) = (1 - x)^{-\delta} f_0(x), \quad \theta_1(x) = (1 - x)^{-\delta} f_1(x).$$

The ODE system satisfied by $f_0$ and $f_1$ is then

$$\begin{cases} (x - 1)f_0' + (3 - q - \delta)f_0 + (q - 2)f_1 = 0 \\ 2x(x - 1)f_1' - [1 + \eta_1 + (\eta_1 + 2q - 7 + 2\delta)x]\,f_1 + (\eta_1 - 3 + q)f_0 = 0. \end{cases} \tag{4.14}$$

The form of the equation coefficients suggests we define $\delta'$ as,

$$\delta' := \delta + q - 3, \tag{4.15}$$

so that

$$\begin{cases} (x - 1)f_0' - \delta' f_0 + (q - 2)f_1 = 0 \\ 2x(x - 1)f_1' - \left(1 + \eta_1 + (\eta_1 - 1 + 2\delta')x\right)f_1 + (\eta_1 - 3 + q)f_0 = 0. \end{cases} \tag{4.16}$$

From the first equation, we extract $f_1$ as a function of $f_0$ and $f_0'$ for $q \neq 2$,

$$f_1(x) = \frac{x - 1}{2 - q}f_0'(x) - \frac{\delta'}{2 - q}f_0(x), \quad q \neq 2. \tag{4.17}$$

Substituting into (4.16), we obtain the following degree two differential equation satisfied by $f_0$,

$$\frac{2x(x-1)^2}{2-q} f_0''(x) + \left( 2x(x-1)\frac{1-\delta'}{2-q} - \frac{x-1}{2-q}\left(1 + \eta_1 + (\eta_1 - 1 + 2\delta')x\right) \right) f_0'(x)$$

$$+ \left( \eta_1 + q - 3 + \frac{\delta'}{2-q}\left(1 + \eta_1 + (\eta_1 - 1 + 2\delta')x\right) \right) f_0(x) = 0. \qquad (4.18)$$

We want to find $\delta'$ such that this equation reads

$$x(x-1)f_0''(x) + ((a+b+1)x - c)f_0'(x) + abf_0(x) = 0, \qquad (4.19)$$

so that $f_0(x) = {}_2F_1(a, b, c; x)$, the hypergeometric function. This identification shows that $\delta'$ must obey the following relation,

$$E(\delta', \eta_1, q) := 2\delta'(\delta' + \eta_1) + (2-q)(\eta_1 + q - 3) = 0, \qquad (4.20)$$

so that (4.18) simplifies into

$$x(x-1)f_0''(x) + \left( \frac{3 - \eta_1 - 4\delta'}{2}x - \frac{1+\eta_1}{2} \right) f_0'(x) \qquad (4.21)$$

$$- \delta' \frac{1 - \eta_1 - 2\delta'}{2} f_0(x) = 0. \qquad (4.22)$$

This yields

$$a = -\delta', \quad b = \frac{1-\eta_1}{2} - \delta', \quad c = \frac{1+\eta_1}{2}, \qquad (4.23)$$

and we can choose $f_0(x) = {}_2F_1(a, b; c; x)$ and $\theta_0(x) = (1-x)^{-\delta}{}_2F_1(a, b; c; x)$. The other independent solution to the hypergeometric equation is

$$x^{1-c}{}_2F_1(1 + a - c, 1 + b - c; 2 - c; x),$$

which is *non-analytic* at the origin $x = 0$, hence is discarded as a candidate for $f_0$.

Before continuing, let us consider general symmetric Lévy processes: what are the possible couples $(\eta_1, \eta_2)$? We know that we must have $\eta_2 \geq 0$ and the Lévy–Khinchine formula implies that $\eta_1 \geq \eta_2/4$. It happens that every couple $(\eta_1, \eta_2)$ such that $\eta_1 \geq \eta_2/4 \geq 0$ actually corresponds to some (symmetric) Lévy process [2].[1] Moreover, the case $\eta_1 = \eta_2/4$ exactly corresponds to an SLE process, while in the case $\eta_2 = 0$, $L_t$ is a pure jump process with jumps equal to $k\pi$, $k$ odd (notice that the other case is similar with $k$ even, yielding a continuous process on the circle).

For $\eta_2 = 4 - q$, the preceding constraints on $(\eta_1, \eta_2)$ become $q \leq 4$ and $\eta_1 \geq \eta_2/4 = 1 - q/4$, with equality for $\text{SLE}_\kappa$, with $\kappa = 2 - q/2$. Let us then define

$$D_{4-q} := \{(q, \eta_1) \in \mathbb{R}^2; q \leq 4, \eta_1 \geq 1 - q/4\}. \qquad (4.24)$$

Let us return to Eq. (4.20). It can be shown (see below) that $\eta_1^2 - 2(2-q)(\eta_1 + q - 3) \geq 0$ in $D_{4-q}$; we may thus extract $\delta'$ from (4.20):

$$\delta_\pm = \delta'_\pm + 3 - q$$

_____

[1]Rémy Rhodes, private communication.

$$\delta'_\pm = \delta'_\pm(q, \eta_1) := \frac{1}{2}\left(-\eta_1 \pm \sqrt{\eta_1^2 - 2(2-q)(\eta_1 + q - 3)}\right). \tag{4.25}$$

Replacing in (4.23) $\delta'$ by its value in terms of $\eta_1, q$, we get:

$$a_\pm = a_\pm(\eta_1, q) := \frac{1}{2}\eta_1 \mp \frac{1}{2}\sqrt{\eta_1^2 - 2(2-q)(\eta_1 + q - 3)} \tag{4.26}$$

$$b_\pm = b_\pm(\eta_1, q) := \frac{1}{2} \mp \frac{1}{2}\sqrt{\eta_1^2 - 2(2-q)(\eta_1 + q - 3)} \tag{4.27}$$

$$c = c(\eta_1, q) := \frac{1 + \eta_1}{2}. \tag{4.28}$$

We can now compute $f_1$ as,

$$\begin{aligned} f_1(x) &= \frac{x-1}{2-q}f_0'(x) + \frac{-\delta'}{2-q}f_0(x) \\ &= \frac{a}{2-q}\,_2F_1(a, b; c; x) + \frac{ab(x-1)}{c(2-q)}\,_2F_1(a+1, b+1; c+1; x). \end{aligned} \tag{4.29}$$

Using expression (4.7) for the integral means, we get

$$\frac{1}{2\pi}I(r) = (1 - r^2)^{-\delta}\left[(1 + r^2)f_0(r^2) - 2r^2 f_1(r^2)\right]. \tag{4.30}$$

**4.1.1. The (+)-Branch.** Let us first consider the case where

$$a = a_+, \ b = b_+.$$

We then have $c - a_+ - b_+ = \sqrt{\eta_1^2 - 2(2-q)(\eta_1 + q - 3)} > 0$, so that

$$0 < \,_2F_1(a, b; c; 1) = \frac{\Gamma(c)\Gamma(c - a - b)}{\Gamma(c - a)\Gamma(c - b)} < \infty. \tag{4.31}$$

If furthermore, $a + b + 1 < c$, then $\,_2F_1(a+1, b+1; c+1; 1) < \infty$, and

$$\Delta := \lim_{r \to 1}\left((1 + r^2)f_0(r^2) - 2r^2 f_1(r^2)\right) = 2\left(1 - \frac{a}{2-q}\right)\,_2F_1(a, b; c; 1) < \infty.$$

We have thus proven that if $\Delta > 0$, the spectrum is

$$\beta(2, q) = 3 - q + \delta'_+(\eta_1, q) = 3 - q + \frac{1}{2}\left(\sqrt{\eta_1^2 - 2(2-q)(\eta_1 + q - 3)} - \eta_1\right).$$

One can check that the coefficient $A := 1 - a_+/(2 - q) > 0$ for $q < 3$, whereas for $q \geq 3$, it vanishes for $\eta_1 = 1 - q$ or $\eta_1 = 3 - q$. In $D_{4-q}$, $A$ is thus positive since $\eta_1 \geq 1 - q/4$ is located outside the non-positive interval $[1 - q, 3 - q]$. So we get that the spectrum is equal to $\delta_+$ on the subset of $D_{4-q}$ of points for which $a + b + 1 < c$. This condition is just $Z > 1$, with

$$Z = Z(\eta_1, q) := \eta_1^2 - 2(2 - q)(\eta_1 + q - 3). \tag{4.32}$$

Note that $Z$ can be written as

$$Z = (q - 3)^2 + (\eta_1 + q - 2)^2 - 1 \tag{4.33}$$

$$= X^2 + Y^2 - 1, \quad X := q - 3, \quad Y := \eta_1 + q - 2, \tag{4.34}$$

so that the condition $Z > 1$ corresponds to the *exterior* of the **blue ellipse** of equation $Z = 1$, i.e., $X^2 + Y^2 = 2$ in the $(q, \eta_1)$-plane (Fig. 12).

Notice that the set $Z = 0$ is the co-centered **green ellipse** of equation $X^2 + Y^2 = 1$, which only intersects $D_{4-q}$ at the tangency point $(\frac{12}{5}, \frac{2}{5})$ with the $(\eta_1 = 1 - q/4)$-line, implying that $Z \geq 0$ in $D_{4-q}$, as mentioned above.

In the *interior* of the blue ellipse, we instead have $a + b < c < a + b + 1$, and we use the Euler transformation,

$$_2F_1(a, b; c; x) = (1 - x)^{c-a-b} \, _2F_1(c - a, c - b; c; x), \qquad (4.35)$$

so that

$$_2F_1(a + 1, b + 1; c + 1; x) = (1 - x)^{c-a-b-1} \, _2F_1(c - a, c - b; c + 1; x). \tag{4.36}$$

We then get from (4.29)

$$f_1(x) = \frac{a}{2 - q} \, _2F_1(a, b; c; x) - \frac{ab}{c} \frac{1}{(2 - q)} (1 - x)^{c-a-b} \, _2F_1(c - a, c - b; c + 1; x). \tag{4.37}$$

We now have $_2F_1(a, b; c; 1) < \infty$ and $_2F_1(c - a, c - b; c + 1; 1) < \infty$, so the second term in (4.39) still vanishes as $x \to 1$. This again yields

$$0 < \Delta = 2 \left( 1 - \frac{a}{2 - q} \right) \, _2F_1(a, b; c; 1) < \infty,$$

i.e., the same result as found outside the blue ellipse. We thus find for the $(+)$-branch,

$$\frac{1}{2\pi} I(r) \sim 2(1 - r^2)^{-\delta_+} \left[ 1 - \frac{a_+}{2 - q} \right] \frac{\Gamma(c)\Gamma(c - a_+ - b_+)}{\Gamma(c - a_+)\Gamma(c - b_+)}, \quad r \to 1^-, \quad q \neq 2. \tag{4.38}$$

**4.1.2. The $(-)$-Branch.** Let us now consider the other possible choice,

$$a = a_-, \; b = b_-.$$

We then use both (4.35) and (4.36) in (4.29),

$$f_1(x) = (1 - x)^{c-a-b}$$
$$\left[ \frac{a}{2 - q} \, _2F_1(c - a, c - b; c; x) - \frac{ab}{c} \frac{1}{(2 - q)} \, _2F_1(c - a, c - b; c + 1; x) \right], \tag{4.39}$$

where now $c - a - b < 0$, and where

$$_2F_1(c - a, c - b; c; 1) = \frac{\Gamma(c)\Gamma(a + b - c)}{\Gamma(a)\Gamma(b)} < \infty,$$

$$_2F_1(c - a, c - b; c + 1; 1) = \frac{\Gamma(c + 1)\Gamma(a + b - c + 1)}{\Gamma(a + 1)\Gamma(b + 1)} < \infty.$$

From the well-known identity $\Gamma(x + 1) = x\Gamma(x)$, we finally get for (4.39)

$$f_1(x) = (1 - x)^{c-a-b} \frac{c - b}{2 - q} \frac{\Gamma(c)\Gamma(a + b - c)}{\Gamma(a)\Gamma(b)}.$$

$I(r)$ (4.30) is now equivalent for $r^2 = x \to 1$ to

$$\frac{1}{2\pi} I(r) \sim 2(1-x)^{-\delta_- + c - a - b} \left[ 1 - \frac{c-b}{2-q} \right] \frac{\Gamma(c)\Gamma(a+b-c)}{\Gamma(a)\Gamma(b)}.$$

where we recall that $a = a_-, b = b_-$. We now use the *duality* formulae

$$c - a_- = b_+, \ c - b_- = a_+, \ a_- + b_- - c = c - a_+ - b_+,$$

and

$$\delta_\pm = 3 - q + \delta'_\pm, \ \delta'_- - \delta'_+ = c - a_- - b_-,$$

so that for $r \to 1^-$,

$$\frac{1}{2\pi} I(r) \sim 2(1-r^2)^{-\delta_+} \left[ 1 - \frac{a_+}{2-q} \right] \frac{\Gamma(c)\Gamma(c - a_+ - b_+)}{\Gamma(c - a_+)\Gamma(c - b_+)},$$

which is exactly the same as the result (4.38) for the (+)-choice in Sect. 4.1.1.

*Remark 4.1.* **The $q = 2$ case.** Up to now, we have assumed that $q \neq 2$. The solution for $q = 2$, thus $\eta_2 = 2, \eta_1 \geq 1/2$, can be obtained by continuity as the $q \to 2$ limit of $f_0$ and $f_1$ (4.17). Equation (4.26) gives:

$$a_+ = \frac{1}{2\eta_1}(\eta_1 - 1)(q - 2) + \mathcal{O}\left((q-2)^2\right),$$

$$b_+ = \frac{1}{2}(1 - \eta_1) + \mathcal{O}(q - 2), \quad c = \frac{1}{2}(1 + \eta_1),$$

so that $f_0 = 1$, and (4.17) has a finite limit when $q \to 2$,

$$f_1(x) = \frac{\eta_1 - 1}{2\eta_1} \left[ 1 - \frac{1 - \eta_1}{1 + \eta_1}(1 - x) \, {}_2F_1(1, \tfrac{1}{2}(3 - \eta_1); \tfrac{1}{2}(3 + \eta_1); x) \right],$$

$$(4.40)$$

together with $\delta'_+ = 0$ and $\delta_+ = 1$. Equation (4.38) simply becomes $\frac{1}{2\pi} I(r) \sim (1 - r^2)^{-1} (3 - 1/\eta_1)$, as $r \to 1^-$, so that $\beta(p = 2, q = 2) = 1$.

We have therefore proved the following

**Theorem 4.1.** *For a Lévy process, with symbols $\eta_2 = 4 - q$, $\eta_1 \geq \eta_2/4$ for $q \leq 4$, the generalized integral means spectrum of the corresponding LLE is:*

$$\beta(2, q) = 3 - q + \frac{1}{2} \left( \sqrt{\eta_1^2 - 2(2 - q)(\eta_1 + q - 3)} - \eta_1 \right). \qquad (4.41)$$

*In particular, if $q = 2, \eta_2 = 2$, the standard integral means spectrum at $p = 2$ of the logarithm of the LLE is independent of $\eta_1 \geq 1/2$ and equal to $\beta(2, 2) = 1$.*

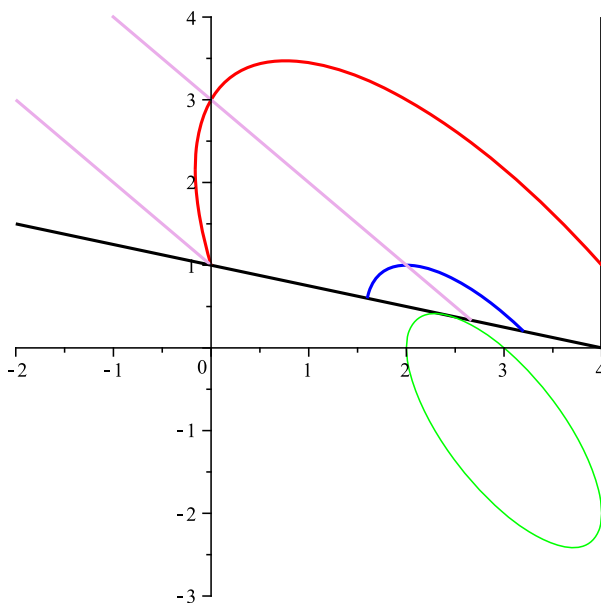In the $q = 0$ case, Eq. (4.41) recovers a result of [50].

FIGURE 12. Domain lines in the $(q, \eta_1)$ plane, for the $\eta_2 = 4 - q$ case. The two purple straight lines have for equations, $\eta_1 = 1 - q$ and $\eta_1 = 3 - q$. The green, blue and red ellipses have for respective equations $X^2 + Y^2 = 1, 2, 10$, with $X = q - 3, Y = \eta_1 + q - 2$, with same center located at $(q, \eta_1) = (3, -1)$

**4.1.3. Algebraic Solutions.** As a transition to the next section, let us look for purely algebraic solutions of the form,

$$\theta_j(x) = (1 - x)^{-\alpha} f_j(x), \quad f_j(x) = A_j^0 + A_j^1(1 - x), \ j = 0, 1.$$

where $A_j^k, k = 0, 1$ are fixed coefficients and with the understanding that $\theta_j = 0$ for $j \geq 2$. Recall that the hypergeometric function $_2F_1$ is given by the well-known series expansion,

$$_2F_1(a, b; c; x) = \sum_{n=0}^{\infty} \frac{(a)_n (b)_n}{(c)_n} \frac{x^n}{n!} = 1 + \frac{ab}{c} \frac{x}{1!} + \frac{a(a+1)b(b+1)}{c(c+1)} \frac{x^2}{2!} + \cdots,$$

$$(4.42)$$

with

$$(a)_n = \begin{cases} 1 & n = 0 \\ a(a+1) \cdots (a + n - 1) & n \geq 1, \end{cases}$$

so that the fact that $f_0(x) = {}_2F_1(a, b; c; x)$ is at most linear in $x$ implies that either: $a = a_+ = 0$; $a_+ = -1$; $b = b_+ = 0$; or $b_+ = -1$. The function $f_1$ (4.17)

is then also linear, assuming for now that $q \neq 2$. For later convenience, let us write (4.26) (4.27) as

$$a_+ = \tfrac{1}{2}\eta_1 - \tfrac{1}{2}Z^{1/2}, \quad b_+ = \tfrac{1}{2} - \tfrac{1}{2}Z^{1/2},$$
$$Z = \eta_1^2 - 2(2-q)(\eta_1 + q - 3). \tag{4.43}$$

- **The $a_+ = 0$ case.** The equation $Z = \eta_1^2$ gives for $q \neq 2$, $\eta_1 = 3 - q$, which recovers the algebraic solutions, Eqs. (4.10) and (4.11). For $q = 2$, Remark (4.1) and Eq. (4.40) yield for $\eta_1 = 1$, $f_0 = 1$, $f_1 = 0$, in agreement with (4.11).
- **The $a_+ = -1$ case.** The equation $Z = (\eta_1 + 2)^2$ yields $(4 - q)(\eta_1 + q - 1) = 0$. Hence we first recover the algebraic case $\eta_1 = 1 - q$, as in Eqs. (4.12) and (4.13). The other case, $q = 4$, is the vertical boundary line for $D_{4-q}$ (Fig 12), where $\eta_2 = 0$, and for which Eq. (4.41) gives $\delta_+ = \beta(p = 2, q = 4) = 0$, so that $\theta_j = f_j$, $j = 0, 1$. One further finds $b_+ = -c = -\tfrac{1}{2}(1 + \eta_1)$, so that one gets the polynomial solutions, $f_0(x) = {}_2F_1(-1, b_+; c; x) = 1 + x$, and from (4.17) $f_1(x) = \tfrac{1}{2}(1 + x)$.
- **The $b_+ = 0$ case.** From (4.43), we get the condition $Z = 1$, which in parameterization (4.33) of $Z$ (4.32) is just that defining the **blue ellipse** as $X^2 + Y^2 = 2$. Its solution is given by $\eta_1 = 2 - q \pm \sqrt{-q^2 + 6q - 7}$. The condition $(q, \eta_1) \in D_{4-q}$ (4.24) selects the (+)-branch only and restricts the range of parameter $q$ to $q \in [\tfrac{8}{5}, \tfrac{16}{5}]$ (see Fig. 12). This yields a first line of algebraic solutions,

$$\begin{cases} \eta_1 & = 2 - q + \sqrt{1 + (q-2)(4-q)} \\ \beta(2,q) & = \tfrac{1}{2}\left(5 - q - \sqrt{1 + (q-2)(4-q)}\right) \\ q & \in [\tfrac{8}{5}, \tfrac{16}{5}]. \end{cases}$$

- **The $b_+ = -1$ case.** From (4.43), we get the condition $Z = 9$, which in parameterization (4.33) is defining a **red ellipse** as $X^2 + Y^2 = 10$. Its solution is given by $\eta_1 = 2 - q \pm \sqrt{1 + 6q - q^2}$. The condition $(q, \eta_1) \in D_{4-q}$ (4.24) allows for both ($\pm$)-branches, but restricts the range of parameter $q$ to $[3 - \sqrt{10}, 4]$ for the (+)-branch, and to $[3 - \sqrt{10}, 0]$ for the (−)-branch (see Fig. 12). This finally gives algebraic solutions for

$$\begin{cases} \eta_1 & = 2 - q + \sqrt{1 + 6q - q^2} \\ \beta(2,q) & = \tfrac{1}{2}(7 - q - \sqrt{1 + 6q - q^2}) \\ q & \in [3 - \sqrt{10}, 4], \end{cases}$$

and

$$\begin{cases} \eta_1 & = 2 - q - \sqrt{1 + 6q - q^2} \\ \beta(2,q) & = \tfrac{1}{2}(7 - q + \sqrt{1 + 6q - q^2}) \\ q & \in [3 - \sqrt{10}, 0]. \end{cases}$$

From (4.42) and for $n \geq 2$, one further finds a whole series of algebraic solutions where the $f_j$'s are *polynomials of degree $n$*, when either $(a)_{n+1} = 0$ or $(b)_{n+1} = 0$, i.e., either $a_+ = -n$ or $b_+ = -n$.

- **The $a_+ = -n$ case**. From (4.43), one finds:

$$\eta_1 = \frac{(2-q)(3-q) - 2n^2}{2 - q + 2n}. \qquad (4.44)$$

One recovers the two linear cases seen above, $n = 0$, $\eta_1 = 3 - q$ with $q \le 8/3$ and $n = 1$, $\eta_1 = 1 - q$ with $q \le 0$. For $n \ge 2$, the Lévy symbol condition $\eta_1 \ge 1 - q/4$ requires that $q \le 2 - 2n$. Equation (4.44) can be recast as

$$(2 - q + 2n)(\eta_1 + q - 3 + 2n) = 2n(n-1).$$

This corresponds to a branch of a **hyperbola** $\mathcal{H}_n$ in the $(q, \eta_1)$ plane, defined in affine coordinates by

$$X_n Y_n = 2n(n-1), \quad X_n := 2 - q + 2n,$$
$$Y_n := \eta_1 + q - 3 + 2n, \quad q \le 2 - 2n, \ n \ge 2. \qquad (4.45)$$

- **The $b_+ = -n$ case**. From (4.43), one readily finds

$$Z = (2n + 1)^2, \qquad (4.46)$$

which in parameterization (4.33) is defining the **ellipse** $\mathcal{E}_n$ by the equation

$$X^2 + Y^2 = 1 + (2n + 1)^2.$$

This in turn yields

$$\eta_1 = 2 - q \pm \sqrt{(2-q)(q-4) + (2n+1)^2}, \qquad (4.47)$$

together with

$$\beta(2, q) = 3 - q + \frac{1}{2}(2n + 1 - \eta_1)$$
$$= \frac{1}{2}\left(2n + 5 - q \mp \sqrt{(2-q)(q-4) + (2n+1)^2}\right). \qquad (4.48)$$

The condition $(q, \eta_1) \in D_{4-q}$ (4.24) allows for both $(\pm)$-branches, but restricts for the $(+)$-branch the range of parameter $q$ to $[3 - \sqrt{(2n+1)^2 + 1}, 4]$, and for the $(-)$-branch to $[3 - \sqrt{(2n+1)^2 + 1}, \frac{8}{5}(1 - n)]$. For $n = 0, 1$ one recovers the blue and red ellipses of Fig. 12.

Let us finally investigate what happens on the boundary of $D_{4-q}$.

(1) *On the $\eta_1 = 1 - q/4$ line:*
As we have already seen, this case occurs when $\eta_2 = 4\eta_1$ and the process is an SLE$_\kappa$ with $\kappa = 2\eta_1 = 2 - q/2$, for which we get from the above,

$$\begin{cases} \beta(2, q) & = 1 - \frac{1}{4}q, \ q \ge \frac{12}{5}, \\ & = 4 - \frac{3}{2}q, \ q \le \frac{12}{5}. \end{cases} \qquad (4.49)$$

It is known that the SLE generalized spectrum has several phases [15], among which the standard 'bulk' spectrum [10],

$$\beta_0(p; \kappa) := -p + \frac{(4+\kappa)^2}{4\kappa} - \frac{\kappa + 4}{4\kappa}\sqrt{(4+\kappa)^2 - 8\kappa p}, \qquad (4.50)$$

and the 'unbounded whole-plane' one [15],

$$\beta_1(p, q; \kappa) := 3p - 2q - \frac{1}{2} - \frac{1}{2}\sqrt{1 + 2\kappa(p - q)}. \tag{4.51}$$

We thus have

$$\begin{cases} \beta_0(2; \kappa = 2 - q/2) & = 1 - \frac{1}{4}q, \ q \geq -4, \\ & = \frac{16}{4-q}, \ q \leq -4. \\ \beta_1(2, q; \kappa = 2 - q/2) & = 4 - \frac{3}{2}q, \ q \leq 3, \\ & = 7 - \frac{5}{2}q, \ q \geq 3. \end{cases}$$

Hence, on the SLE boundary line, a *phase transition* takes place at $q = 12/5$ in the spectrum (4.49), in the sense that $\beta(2, q) = \beta_1(2, q; \kappa = 2 - q/2)$ if $q \leq 12/5$ and $\beta(2, q) = \beta_0(2; \kappa = 2 - q/2)$ if $q \geq 12/5$. One can check that the phase transition point $(p = 2, q = 12/5)$ is located on the so-called green parabola that delineates the respective domains of validity of $\beta_0$ and $\beta_1$ for whole-plane $\text{SLE}_{\kappa=4/5}$ [15, Sec. 5.2.2].

(2) *On the $q = 4$ line:*
Here, $\eta_2 = 0$ and the spectrum is $\beta(2, 4) = 0, \forall \eta_1$. This case corresponds to a pure jump Lévy process, whereas the equality $q = 2p = 4$ corresponds to a bounded LLE process [15]; the above result then agrees with [11].

Figure 12 summarizes the results of this section, showing

- the domain $D_{4-q}$, domain of validity of the hypergeometric analysis;
- the domain of definition of the square root involved in the expression of the spectrum $\beta(2, q)$ (4.41), which is the exterior of the **green** ellipse (thus containing $D_{4-q}$);
- the $\eta_1 = 1 - q$ and $\eta_1 = 3 - q$ lines, corresponding to degenerate hypergeometric solutions with $a_+ = -1, 0$;
- the special solutions with $b_+ = -1, 0$, for which the hypergeometric $f_0, f_1$ are degree 1 polynomials, which, respectively, correspond to the two **red** and **blue** ellipses (intersected with $D_{4-q}$). Note that the phase-transition point $(q = 12/5, \eta_1 = 2/5)$ is the intersection point of the boundary of $D_{4-q}$ with the **green** ellipse (a single tangency point).

## 4.2. The $\eta_2 = -q$ Case

Here the points $(q, \eta_1)$ must belong to

$$D_{-q} = \{(q, \eta_1) : q \leq 0, \ \eta_1 \geq -q/4\}. \tag{4.52}$$

In this case, the first three equations (4.4) together with (4.5) form a system of coupled ODEs with unknowns $\theta_j, j = 0, 1, 2$,

$$\begin{cases} (\xi - 1)\theta_0'(\xi) - (q - 3)\theta_0(\xi) + (q - 2)\theta_1(\xi) = 0, \\ 2\xi(\xi - 1)\theta_1'(\xi) - [\eta_1 + 1 + (\eta_1 + 2q - 7)\xi]\,\theta_1(\xi) + (\eta_1 + q - 3)\theta_0(\xi) \\ +(\eta_1 + q - 1)\xi\theta_2(\xi) = 0, \\ 2\xi(\xi - 1)\theta_2'(\xi) - [2 - q + (q - 8)\xi]\,\theta_2(\xi) - 4\theta_1(\xi) = 0. \end{cases}$$
$$\tag{4.53}$$

**4.2.1. Polynomial Ansatz.** Let us now consider for $n \geq 0$ the following *Ansatz*,

$$\theta_j(\xi) = (1 - \xi)^{-\alpha} f_j(\xi),$$

$$f_j(\xi) = \sum_{k=0}^{n} A_j^k P_k(\xi), \quad P_k(\xi) := (1 - \xi)^k, \ j = 0, 1, 2. \qquad (4.54)$$

Eqs. (4.53) give

$$\begin{cases} [1] \bullet \ (\xi - 1)f_0'(\xi) - (q - 3 + \alpha)f_0(\xi) + (q - 2)f_1(\xi) = 0, \\ [2] \bullet \ 2\xi(\xi - 1)f_1'(\xi) - [\eta_1 + 1 + (\eta_1 + 2\alpha + 2q - 7)\xi] f_1(\xi) \\ \quad + (\eta_1 + q - 3)f_0(\xi) + (\eta_1 + q - 1)\xi f_2(\xi) = 0, \\ [3] \bullet \ 2\xi(\xi - 1)f_2'(\xi) - [2 - q + (2\alpha + q - 8)\xi] f_2(\xi) - 4f_1(\xi) = 0. \end{cases} \qquad (4.55)$$

Consider then in each left-hand side of the three equations [1], [2], [3] in (4.55), the contributions arising for a *fixed* $k$ from the monomials $A_j^k P_k$ in $f_j, j = 0, 1, 2$ (4.54). Because of the universal presence of factors $(\xi - 1)$ or $\xi(\xi - 1)$ in front of derivatives $P_k'(\xi) = -kP_{k-1}(\xi)$, and of polynomials of degree at most 1 in $\xi$ in front of $P_k(\xi)$, only $P_k$ and $P_{k+1}$ monomials will result from $P_k$. We explicitly find for the three lines the resulting contributions,

$$\begin{cases} [1] \bullet \ \left\{[k - (q - 3 + \alpha)]A_0^k + (q - 2)A_1^k\right\} P_k, \\ [2] \bullet \ \left\{(\eta_1 + q - 3)A_0^k + 2[k - (\eta_1 + \alpha + q - 3)] A_1^k + (\eta_1 + q - 1)A_2^k\right\} P_k \\ \quad + \left\{(-2k + \eta_1 + 2\alpha + 2q - 7)A_1^k - (\eta_1 + q - 1)A_2^k\right\} P_{k+1}, \\ [3] \bullet \ \left\{-4A_1^k + [2k - (2\alpha - 6)] A_2^k\right\} P_k + (-2k + 2\alpha + q - 8) A_2^k P_{k+1}. \end{cases} \qquad (4.56)$$

When summing up over $k \in \{0, \cdots, n\}$ to reconstruct the $f_j$'s in (4.55), each monomial $P_k$ must get an overall vanishing coefficient in order to satisfy the equations. Therefore, collecting all coefficients of terms $P_k$, we are led to the recursions,

$$\begin{cases} [1] \bullet \ [k - (q - 3 + \alpha)]A_0^k + (q - 2)A_1^k = 0, \\ [2] \bullet \ (\eta_1 + q - 3)A_0^k + 2[k - (\eta_1 + \alpha + q - 3)] A_1^k + (\eta_1 + q - 1)A_2^k \\ \quad = [2(k - 1) - (\eta_1 + 2\alpha + 2q - 7)]A_1^{k-1} + (\eta_1 + q - 1)A_2^{k-1}, \\ [3] \bullet \ -4A_1^k + 2[k - (\alpha - 3)] A_2^k = [2(k - 1) - (2\alpha + q - 8)] A_2^{k-1}. \end{cases} \qquad (4.57)$$

Note that in the $k = 0$ case, there are *no* $A_1^{k-1}$ and $A_2^{k-1}$ terms, which are thus set by convention equal to 0.

This system is best written under a matricial form, by defining successively,

$$D_k(\alpha) := \begin{pmatrix} k - (\alpha + q - 3) & q - 2 & 0 \\ \eta_1 + q - 3 & 2k - 2(\eta_1 + \alpha + q - 3) & \eta_1 + q - 1 \\ 0 & -4 & 2k - 2(\alpha - 3) \end{pmatrix}$$

and

$$C_{k-1}(\alpha) := \begin{pmatrix} 0 & 0 & 0 \\ 0 & 2(k-1) - (\eta_1 + 2\alpha + 2q - 7) & \eta_1 + q - 1 \\ 0 & 0 & 2(k-1) - (2\alpha + q - 8) \end{pmatrix}.$$

Let us finally define the column vectors,

$$\mathbf{A}^k := \begin{pmatrix} A_0^k \\ A_1^k \\ A_2^k \end{pmatrix}, \quad k \geq 0,$$

so that recursions (4.57) become for $k \geq 1$

$$D_k(\alpha)\mathbf{A}^k = C_{k-1}(\alpha)\mathbf{A}^{k-1}, \quad k \geq 1, \tag{4.58}$$

together with the initial condition,

$$D_0(\alpha)\mathbf{A}^0 = \mathbf{0}, \tag{4.59}$$

and the closure relation

$$\mathbf{A}^{n+1} = \mathbf{0}, \tag{4.60}$$

such that $\mathbf{A}^k = \mathbf{0}, \ \forall k \geq n + 1$.

Equation (4.59) shows that for a non-trivial solution to exist, one must have

$$\det D_0(\alpha) = 0,$$

with $\mathbf{A}^0$ an eigenvector of vanishing eigenvalue. The determinant of $D_0$ is

$$\det D_0(\alpha) = 2(1 - \alpha)E_0(\alpha)$$
$$E_0(\alpha) := 2(\alpha + q - 3)(\eta_1 + \alpha + q - 5) - q(\eta_1 + q - 3). \tag{4.61}$$

Let us look for the solutions to

$$E_0(\alpha) = 0 \Leftrightarrow \alpha = \alpha_0^\pm := 3 - q + \frac{1}{2}\left(2 - \eta_1 \pm \sqrt{\hat{Z}}\right), \tag{4.62}$$

$$\hat{Z} = \hat{Z}(\eta_1, q) := (\eta_1 - 2)^2 + 2q(\eta_1 + q - 3), \tag{4.63}$$

which yields the set of non-trivial zeroes of $\det D_0$. $\hat{Z}$ can also be written as:

$$\hat{Z} = (q - 1)^2 + (\eta_1 + q - 2)^2 - 1$$
$$= \hat{X}^2 + Y^2 - 1, \quad \hat{X} := q - 1, \quad Y := \eta_1 + q - 2. \tag{4.64}$$

Thus, $\hat{Z}$ is nonnegative outside the **green** ellipse $\hat{Z} = 0$ (Fig. 13), and since $q \leq 0$ in $D_{-q}$, expression (4.64) is clearly non-negative there, vanishing only for $q = 0, \eta_1 = 2$, so that $\alpha_0^\pm$ (4.62) is defined and real in $D_{-q}$. Observe also that a translation maps $Z$ (4.33) to $\hat{Z}$ (4.64),

$$\hat{Z}(\eta_1, q) = Z(\eta_1 - 2, q + 2). \tag{4.65}$$

The null eigenvectors $\mathbf{A^0}(\alpha)$ of $D_0(\alpha)$ with vanishing eigenvalue are given, either for $\alpha = \alpha_0^\pm$ or for $\alpha = 1$, by the one-dimensional space

$$\mathbf{A^0} = \mathbf{A^0}(\alpha) = \begin{cases} A_0^0 \in \mathbb{R} \\ A_1^0 = \frac{1}{q-2}(\alpha + q - 3)A_0^0 \\ A_2^0 = -\frac{2}{\alpha-3}A_1^0. \end{cases} \tag{4.66}$$

As it will appear shortly, the value of the generalized spectrum is given by the root $\alpha_0^+$ in (4.62). To check this, consider the first integrability line, $\eta_1 = 3 - q$, where (4.62) gives,

$$\begin{cases} \alpha_0^+ &= 3 - q, \quad \alpha_0^- = 2, \qquad q \le 1 \\ &= 2 \qquad\qquad = 3 - q, \quad q \ge 1. \end{cases}$$

Therefore, the choice of root $\alpha_0^+$ reproduces for $q \le 1$, hence $q \le 0$ in $D_{-q}$ the expected spectrum (4.11) $\beta(2, q) = 3 - q$. For the second integrability line, $\eta_1 = 1 - q$, one similarly finds

$$\begin{cases} \alpha_0^+ &= 4 - q, \quad \alpha_0^- = 3, \qquad q \le 1 \\ &= 3 \qquad\qquad = 4 - q, \quad q \ge 1. \end{cases}$$

The condition $\eta_1 \ge 0$ requires that $q \le 1$; thus, the choice of root $\alpha_0^+$ again gives for $q \le 0$ in $D_{-q}$ the expected spectrum (4.13) $\beta(2, q) = 4 - q$.

**4.2.2. Recursion.** Assume for the time being that for $k \ge 1$, $\det D_k(\alpha) \ne 0$, so that $D_k(\alpha)$ is invertible. We immediately get from (4.58)

$$\mathbf{A}^k = M_k \mathbf{A}^0$$

$$M_k = \prod_{\ell=0}^{k-1} D_{k-\ell}^{-1}(\alpha)C_{k-\ell-1}(\alpha) \tag{4.67}$$

$$:= D_k^{-1}(\alpha)C_{k-1}(\alpha)D_{k-1}^{-1}(\alpha)C_{k-2}(\alpha)\cdots D_1^{-1}(\alpha)C_0(\alpha). \tag{4.68}$$

Notice that $D_k$ and $C_k$ obey a simple *shift* relation,

$$D_k(\alpha) = D_0(\alpha - k), \quad C_k(\alpha) = C_0(\alpha - k). \tag{4.69}$$

Result (4.68) can then be rewritten simply as

$$M_k = \prod_{\ell=0}^{k-1} D_0^{-1}(\alpha - k + \ell)C_0(\alpha - k + \ell + 1)$$

$$:= D_0^{-1}(\alpha - k)C_0(\alpha - k + 1)D_0^{-1}(\alpha - k + 1)C_0(\alpha - k + 2)\cdots$$
$$D_0^{-1}(\alpha - 1)C_0(\alpha). \tag{4.70}$$

**4.2.3. Polynomial Solutions.** Requiring the $f_j$'s to be polynomials of given degree $n \ge 1$ is equivalent to requiring that $\mathbf{A}^{n+1} = \mathbf{0}$ (4.60). From (4.58), we get

$$D_{n+1}(\alpha)\mathbf{A}^{n+1} = C_n\mathbf{A}^n = \mathbf{0},$$

i.e.,

$$[2n - (\eta_1 + 2\alpha + 2q - 7)]A_1^n + (\eta_1 + q - 1)A_2^n = 0, \tag{4.71}$$
$$[2n - (2\alpha + q - 8)]A_2^n = 0. \tag{4.72}$$

If $2n - (2\alpha + q - 8) \neq 0$, then $A_2^n = 0$, and for a non-vanishing solution to exist, one needs the condition $2n - (\eta_1 + 2\alpha + 2q - 7) = 0$ to hold for $\alpha = \alpha_0^{\pm}$. This gives $\pm\sqrt{\hat{Z}} = 2n - 1$, with $n \geq 1$. This selects the $(+)$-branch $\alpha = \alpha_0^+$, together with

$$\hat{Z} = (2n - 1)^2, \ n \geq 1. \tag{4.73}$$

Because of (4.64), one thus finds from (4.73) a set of **ellipses** $\hat{\mathcal{E}}_n$ in the $(q, \eta_1)$ plane, satisfying the equation

$$\hat{X}^2 + Y^2 = (2n - 1)^2 + 1. \tag{4.74}$$

It is interesting to note that it is far from obvious that condition (4.73), while necessary, is also *sufficient* to obtain that $A_2^n = 0$ at level $n$ of recursion (4.67), when starting from eigenvector $\mathbf{A}^0(\alpha)$ (4.66) for $\alpha = \alpha_0^+$. We checked with **Mathematica®** that this is indeed the case, but despite repeated attempts, a combinatorial-like proof has eluded us.

*Remark 4.2.* Degeneracy of $D_k(\alpha)$. Let us finally consider the degenerate case when $\det D_k(\alpha) = \det D_0(\alpha - k) = 0$. Since $\alpha = \alpha_0^+$, this requires that either $\alpha_0^+ - k = \alpha_0^-$ or $\alpha_0^+ - k = 1$.

- **Case** $\alpha_0^+ - k = \alpha_0^-$. This gives $\hat{Z} = k^2$, and since $\hat{Z} = (2n - 1)^2$, we get $k = 2n - 1$. Since the recursion stops at level $n + 1$, we are only interested in the cases where $k \leq n + 1$, hence $n \leq 2$.

  When $n = 1$, a direct computation gives the solution at level $k = n = 1$ with the necessary condition $A_2^1 = 0$, as $A_1^1 = -\frac{1}{4}(\eta_1 + q - 1)A_2^0$, and $A_0^1 = \frac{q-2}{\alpha+q-4}A_1^1$. Adding to it any null eigenvector of $D_1(\alpha_0^+) = D_0(\alpha_0^-)$ would also provide a solution to the recursion at level $k = 1$, but not its closure at level $n + 1 = 2$. Taking into account the boundary condition, $\theta_0(0) = f_0(0) = A_0^0 + A_0^1 = 1$ yields the explicit solution on ellipse $\hat{\mathcal{E}}_1$,

  $$\theta_j(\xi) = (1 - \xi)^{-\alpha_0^+} f_j(\xi), \ \ f_j(\xi) = A_j^0 + A_j^1(1 - \xi), \ \ j = 0, 1, 2,$$

  $$j = 0: \ A_0^0 = 2\frac{2 - q}{\eta_1 + 1}, \ A_0^1 = \frac{\eta_1 + 2q - 3}{\eta_1 + 1},$$

  $$j = 1: \ A_1^0 = \frac{\eta_1 - 3}{\eta_1 + 1}, \ A_1^1 = \frac{\eta_1 + q - 1}{2 - q}\frac{\eta_1 + q - 3}{\eta_1 + 1},$$

  $$j = 2: \ A_2^0 = \frac{4}{q - 2}\frac{\eta_1 + q - 3}{\eta_1 + 1}, \ A_2^1 = 0.$$

  When $n = 2$, we get $k = n + 1 = 3$. In that case, $\mathbf{A}^3 = \mathbf{0}$ is a trivial solution yielding $\mathbf{A}^k = \mathbf{0}$, $\forall k \geq 3$, and while adding to it any null vector of $D_3(\alpha_0^+)$ would still satisfy the recursion at level 3, it would not close the latter at next levels.

- **Case** $\alpha_0^+ - k = 1$. From (4.62) and (4.73), one finds $\eta_1 = 5 + 2(n-k) - 2q$, and one has to consider the intersection in $D_{-q}$ of this straight line with ellipse $\hat{\mathcal{E}}_n$. One finds two solutions, $q_{n,k}^{\pm} := n - k + 2 \pm \sqrt{\Delta}$, $\Delta = (n-1)^2 + (k-1)(2n+1-k)$. As before, we are only interested in recursion levels $1 \le k \le n+1$, so that $\Delta \ge 0$. One also has $\Delta = (n-k+2)^2 + 2(k-2)(2n+1-k)$, so that for $k \ge 2$, there is one admissible root, $q_{n,k}^- \le 0$, whereas $q_{n,k}^+ \ge 0$, and for $k = 1$, $q_{n,1}^- = 2$, $q_{n,1}^+ = 2n$ which are not in $D_{-q}$. By *continuity*, at points $q_{n,k}^-$ with $2 \le k \le n+1$ on $\hat{\mathcal{E}}_n$, the generalized integral means spectrum is still $\beta(2,q) = \alpha_0^+$.

Equation (4.74) gives for ellipse $\hat{\mathcal{E}}_n$ the equations in Cartesian coordinates $(q, \eta_1) \in D_{-q}$,

$$\begin{cases} \eta_1 = 2 - q + \sqrt{q(2-q) + (2n-1)^2} \\ \alpha = \alpha_0^+ = \beta(2,q) = \frac{1}{2}(5 - q + 2k - \sqrt{q(2-q) + (2n-1)^2}) \\ q \in \left[1 - \sqrt{1 + (2n-1)^2}, 0\right], \end{cases} \qquad (4.75)$$

and

$$\begin{cases} \eta_1 = 2 - q - \sqrt{q(2-q) + (2n-1)^2} \\ \alpha = \alpha_0^+ = \beta(2,q) = \frac{1}{2}(5 - q + 2k + \sqrt{q(2-q) + (2n-1)^2}) \\ q \in [1 - \sqrt{1 + (2n-1)^2}, \inf\{-\frac{8}{5}(n - \frac{3}{2}), 0\}]. \end{cases} \qquad (4.76)$$

In the latter set, the $q = -\frac{8}{5}(n - \frac{3}{2})$ point for $n \ge 2$ corresponds to $\mathrm{SLE}_\kappa$ with $\kappa = \frac{4}{5}(n - \frac{3}{2})$ and $\alpha = \beta\left(2, -\frac{8}{5}(n - \frac{3}{2})\right) = \beta_1\left(2, -\frac{8}{5}(n - \frac{3}{2}); \frac{4}{5}(n - \frac{3}{2})\right)$ in (4.51).

The results are summarized in Fig. 13. The **blue** and **red** ellipses in Fig. 13, respectively, correspond to the first $n = 1$ and $n = 2$ cases. Because of (4.65), these ellipses are images by the $(q \to q - 2, \eta_1 \to \eta_1 + 2)$ translation of the corresponding same colour ellipses of Fig. 12 in Sect. 4.1, with a common center now located at $(q, \eta_1) = (1, 1)$. Note also that if the generalized spectrum is given in the whole region $D_{-q}$ by $\alpha_0^+$ in Eq. (4.62), then on the $\mathrm{SLE}_\kappa$-line where $\kappa = 2\eta_1 = \eta_2/2 = -q/2$ it coincides with the spectrum $\beta_1(2,q; \kappa = -q/2) = 5 - 3q/2$, and there is no phase transition along that line, in contrast to the $(\eta_2 = 4 - q)$-case. The phase transition now takes place on the $q = 0 = \eta_2$ line, at its $\eta_1 = 2$ contact point with the green ellipse, since the predicted spectrum $\alpha_0^+$ is there equal to $5 - \eta_1$ for $0 \le \eta_1 \le 2$ and to $3$ for $\eta_1 \ge 2$. This agrees with results (4.13), $\beta(2,0) = 4$ for $\eta_1 = 1$, and (4.11), $\beta(2,0) = 3$ for $\eta_1 = 3$.

*Remark 4.3.* Alternative condition. For completeness, let us also mention that the alternative condition in (4.72), $2n - (2\alpha + q - 8) = 0$ with $\alpha = \alpha_0^{\pm}$, yields $2n + q + \eta_1 = \pm\sqrt{\hat{Z}}$, leading to $\eta_1 + q - 1 = \frac{q(q-2)}{4(n+1)} - n$ and to the selection of the $(+)$-branch. From (4.71), one further needs to check that $(\eta_1 + q + 1)A_1^n = (\eta_1 + q - 1)A_2^n$ upon starting the recursion (4.67) from the null-eigenvector (4.66). Using again **Mathematica**® shows this equality *not* to hold, thus leading to no further solution.
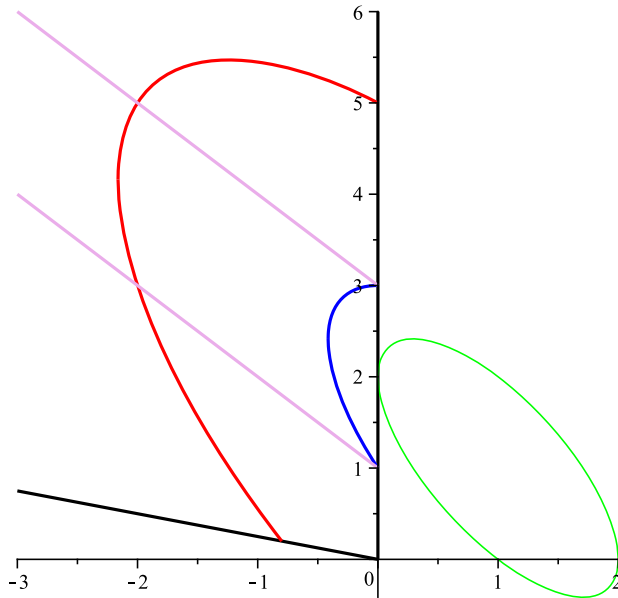
FIGURE 13. Domain lines in the $(q, \eta_1)$ plane, for the $\eta_2 = -q$ case. The two purple straight lines have for equations, $\eta_1 = 1 - q$ and $\eta_1 = 3 - q$. The green, blue and red ellipses have for respective equations $\hat{X}^2 + Y^2 = 1, 2, 10$, with $\hat{X} = q - 1, Y = \eta_1 + q - 2$, with a common center located at $(q, \eta_1) = (1, 1)$

### 4.2.4. General Solution to the Fuchsian System.

From the perspective of Fuchsian systems [39, 50], the initial equations (4.53) for the vector function, $\vartheta(\xi) := (\theta_0(\xi), \theta_1(\xi), \theta_2(\xi))^t$ can be written under the matrix form,

$$\vartheta'(\xi) = \frac{\mathbb{A}}{\xi} \vartheta(\xi) + \frac{\mathbb{B}}{1 - \xi} \vartheta(\xi),$$

where matrices $\mathbb{A}$ and $\mathbb{B}$ do not depend on $\xi$. They are simply given here by

$$\mathbb{A} = \frac{1}{2} \begin{pmatrix} 0 & 0 & 0 \\ \eta_1 + q - 3 & -(\eta_1 + 1) & 0 \\ 0 & -4 & q - 2 \end{pmatrix}, \tag{4.77}$$

$$\mathbb{B} = \frac{1}{2} \begin{pmatrix} 2(3 - q) & 2(q - 2) & 0 \\ \eta_1 + q - 3 & -2(\eta_1 + q - 3) & \eta_1 + q - 1 \\ 0 & -4 & 6 \end{pmatrix}. \tag{4.78}$$

The discriminant of $\mathbb{B}$ is

$$\det(\mathbb{B} - \alpha \mathbb{1}) = (1 - \alpha) \left[ \frac{1}{2}(\eta_1 + q - 3)(2\alpha + q - 6) + (\alpha - 2)(\alpha + q - 3) \right]$$

$$= \frac{1}{2}(1 - \alpha) E_0(\alpha) = \frac{1}{4} \det D_0(\alpha),$$

so that $\mathbb{B}$ has for eigenvalues the zeroes of det $D_0$, $\alpha_0^{\pm}$ (4.62) and 1.

For $\xi \to 1^-$, the vector functions $\vartheta(\xi) = (\theta_0(\xi), \theta_1(\xi), \theta_2(\xi))^t$, have for asymptotic behavior,

$$\vartheta(\xi) = (1-\xi)^{-\alpha_0^+}\mathbf{f}^+(\xi) + (1-\xi)^{-\alpha_0^-}\mathbf{f}^-(\xi) + (1-\xi)^{-1}\mathbf{f}^1(\xi), \quad (4.79)$$

where $\mathbf{f}^{\pm}, \mathbf{f}^1$ are vector functions with Taylor series expansions in $\xi$. In the generic *non-resonant* case, where the eigenvalues do not differ by integer numbers, these functions converge at $\xi = 1$ towards the eigenvectors of $\mathbb{B}$ corresponding to their respective eigenvalue powers $\alpha_0^{\pm}, 1$. In the *resonant* case, they can be polynomials in $\xi$, or can involve polynomials in $-\log(1-\xi)$, which then dominate the limit when $\xi \to 1^-$.

In the resonant case of the $\mathcal{E}_n$ ellipses of Sect. 4.2.3, we have $\alpha_0^- = \alpha_0^+ - (2n-1)$ with $n \geq 1$. These vector functions are then simple polynomials, with

$$\mathbf{f}^+(\xi) = (f_0(\xi), f_1(\xi), f_2(\xi))^t,$$

and $\mathbf{f}^-(\xi) = \mathbf{f}^1(\xi) = \mathbf{0}$. At $\xi = 1$, $\mathbf{f}^+(\xi)$ becomes the eigenvector $\mathbf{f}^+(\xi = 1) = \mathbf{A}_0(\alpha_0^+)$, as given in (4.66).

Let us conclude with the following Theorem.

**Theorem 4.2.** *The generalized integral means spectrum $\beta(2,q)$ of a whole-plane Lévy–Loewner process with Lévy symbols $\eta_1$ and $\eta_2 = -q$ is given in the whole $D_{-q}$ domain (4.52) by $\alpha_0^+$ in Eq. (4.62).*

*Proof.* Because of (4.79), the generalized integral means spectrum must be equal to one of the three eigenvalues $\alpha_0^+, \alpha_0^-, 1$. Eigenvalues $\alpha_0^+$ and $\alpha_0^-$ are equal only when $\hat{Z} = 0$, i.e., on the green ellipse which lies outside $D_{-q}$, except for the point $P_0 = (q = 0, \eta_1 = 2)$. Therefore in $D_{-q}^* := D_{-q} \setminus P_0$, we have $\alpha_0^+ > \alpha_0^-$. One can also check that on $D_{-q}$, $\alpha_0^+ > 1$, whereas the equality $\alpha_0^- = 1$ is realized in $D_{-q}$ on the branch of hyperbola of equation $(\eta_1 + q - 8)(q - 4) = 4$ with $q \leq 0$. We know that $\beta(2,q) = 3 - q = \alpha_0^+$ on the half-line $\eta_1 = 3 - q, q \leq 0$, as well as $\beta(2,q) = 4 - q = \alpha_0^+$ on the half-line $\eta_1 = 1 - q, q \leq 0$. Because of the Hölder inequality, the generalized integral means spectrum is *convex* in $(p,q)$ [15], hence *continuous*. By continuity, $\beta(2,q) = \alpha_0^+$ on these integrability lines cannot jump to $\alpha_0^- < \alpha_0^+$ or $1 < \alpha_0^+$ in $D_{-q}^*$, hence $\beta(2,q) = \alpha_0^+$ in the whole domain. At the singular point $P_0$, the spectrum is still $\alpha_0^+$, with a change of its analytic form. $\qquad\square$

# Acknowledgements

# References

[1] Alberts, T., Binder, I., Viklund, F.: A dimension spectrum for SLE boundary collisions. Commun. Math. Phys. **343**, 273–298 (2016)

[2] Applebaum, D.: Lévy Processes and Stochastic Calculus. Cambridge Studies in Advanced Mathematics, 2nd edn. Cambridge University Press, Cambridge (2009)

[3] Adams, D.A., Sander, L.M., Ziff, R.M.: Harmonic measure for percolation and Ising clusters including rare events. Phys. Rev. Lett. **101**, 144102 (2008)

[4] Binder, I., Duplantier, B.: Multifractal properties of harmonic measure and rotation for Schramm–Loewner evolution (2023) (**in preparation**)

[5] Beliaev, D., Duplantier, B., Zinsmeister, M.: Integral means spectrum of whole-plane SLE. Commun. Math. Phys. **353**(1), 119–133 (2017)

[6] Beliaev, D.: Conformal Maps and Geometry. World Scientific Publishing Europe Ltd, London (2019)

[7] Belikov, A., Gruzberg, I.A., Rushkin, I.I.: Statistics of harmonic measure and winding of critical curves from conformal field theory. J. Phys. A Math. Theor. **41**(28), 285006 (2008)

[8] Binder, I.: Rotational spectrum of planar domains. Ph.D. thesis, California Institute of Technology (1997)

[9] Bettelheim, E., Rushkin, I., Gruzberg, I.A., Wiegmann, P.: Harmonic measure of critical curves. Phys. Rev. Lett. **95**, 170602 (2005)

[10] Beliaev, D., Smirnov, S.: Harmonic measure and SLE. Commun. Math. Phys. **290**(2), 577–595 (2009)

[11] Chen, Z.-Q., Rohde, S.: Schramm–Loewner equations driven by symmetric stable processes. Commun. Math. Phys. **285**, 799–824 (2008)

[12] David, F.: Conformal field theories coupled to 2-D gravity in the conformal gauge. Mod. Phys. Lett. A **3**(17), 1651–1656 (1988)

[13] Duplantier, B., Binder, I.A.: Harmonic measure and winding of conformally invariant curves. Phys. Rev. Lett. **89**, 264101 (2002)

[14] Duplantier, B., Binder, I.A.: Harmonic measure and winding of random conformal paths: a Coulomb gas perspective. Nucl. Phys. B [FS] **802**, 494–513 (2008)

[15] Duplantier, B., Ho, X.H., Le, T.B., Zinsmeister, M.: Logarithmic coefficients and generalized multifractality of whole-plane SLE. Commun. Math. Phys. **359**(3), 823–868 (2018)

[16] Distler, J., Kawai, H.: Conformal field theory and 2D quantum gravity. Nucl. Phys. B **321**, 509–527 (1989)

[17] Duplantier, B., Miller, J., Sheffield, S.: Liouville quantum gravity as a mating of trees. Astérisque **427**, 1–258 (2021)

[18] Duplantier, B., Nguyen, C., Nguyen, N., Zinsmeister, M.: The coefficient problem and multifractality of whole-plane SLE & LLE. Ann. Henri Poincaré **16**(6), 1311–1395 (2015)

[19] Duplantier, B., Rhodes, R., Sheffield, S., Vargas, V.: Renormalization of critical Gaussian multiplicative chaos and KPZ relation. Commun. Math. Phys. **330**(1), 283–330 (2014)

[20] Duplantier, B., Sheffield, S.: Duality and KPZ in Liouville quantum gravity. Phys. Rev. Lett. **102**, 150603 (2009)

[21] Duplantier, B., Sheffield, S.: Liouville quantum gravity and KPZ. Invent. Math. **185**, 333–393 (2011)

[22] Duplantier, B., Sheffield, S.: Schramm–Loewner evolution and Liouville quantum gravity. Phys. Rev. Lett. **107**, 131305 (2011)

[23] Dubédat, J.: Duality of Schramm–Loewner evolutions. Ann. Sci. Éc. Norm. Supér. (4) **42**(5), 697–724 (2009)

[24] Duplantier, B.: Harmonic measure exponents for two-dimensional percolation. Phys. Rev. Lett. **82**, 3940–3943 (1999)

[25] Duplantier, B.: Two-dimensional copolymers and exact conformal multifractality. Phys. Rev. Lett. **82**, 880–883 (1999)

[26] Duplantier, B.: Conformally invariant fractals and potential theory. Phys. Rev. Lett. **84**(7), 1363–1367 (2000)

[27] Duplantier, B.: Higher conformal multifractality. J. Stat. Phys. **110**(3–6), 691–738 (2003)

[28] Duplantier, B.: Conformal fractal geometry & boundary quantum gravity. In: Lapidus, M.L., van Frankenhuysen, M. (Eds.) Fractal Geometry and Applications: A Jubilee of Benoît Mandelbrot, Part 2, Volume 72 of Proceedings of Symposia in Pure Mathematics, pp. 365–482. American Mathematical Society, Providence, RI (2004)

[29] Duplantier, B.: Conformal random geometry. In: Bovier, A., Dunlop, F., den Hollander, F., van Enter, A., Dalibard, J. (eds.) Mathematical Statistical Physics (Les Houches Summer School. Session LXXXIII, 2005), pp. 101–217. Elsevier B.V, Amsterdam (2006)

[30] Frisch, U., Parisi, G.: Turbulence and predictability in geophysical fluid dynamics and climate dynamics. In: Ghil, M., Benzi, R.R., Parisi, G. (eds.) Proceedings of the International School of Physics Enrico Fermi, course LXXXVIII, pp. 84–87. North Holland, New York (1985)

[31] Garnett, J.B., Marshall, D.E.: Harmonic Measure, Volume 2 of New Mathematical Monographs, vol. 2. Cambridge University Press, Cambridge (2008). (**Reprint of the 2005 original**)

[32] Gwynne, E., Miller, J., Sun, X.: Almost sure multifractal spectrum of Schramm–Loewner evolution. Duke Math. J. **167**(6), 1099–1237 (2018)

[33] Hastings, M.B.: Exact multifractal spectra for arbitrary Laplacian random walks. Phys. Rev. Lett. **88**, 055506 (2002)

[34] Halsey, T.C., Jensen, M.H., Kadanoff, L.P., Procaccia, I., Shraiman, B.I.: Fractal measures and their singularities—the characterization of strange sets. Phys. Rev. A **33**, 1141–1151 (1986)

[35] Halsey, T.C., Jensen, M.H., Kadanoff, L.P., Procaccia, I., Shraiman, B.I.: Fractal measures and their singularities: the characterization of strange sets; Erratum: [Phys. Rev. A 33, 1141 (1986)]. Phys. Rev. A **34**, 1601–1601 (1986)

[36] Ho, X.H.: On multifractality, Schwarzian derivative and asymptotic variance of whole-plane SLE. Ph.D. thesis, Université d'Orléans (2016)

[37] Ho, X.H.: Generalized integral means spectrum of SLE. arXiv:2203.10782v1 (2022)

[38] Hentschel, H.G.E., Procaccia, I.: The infinite number of dimensions of probabilistic fractals and strange attractors. Physica D **8**, 435–444 (1983)

[39] Ilyashenko, Y., Yakovenko, S.: Lectures on Analytic Differential Equations. Graduate Studies in Mathematics, vol. 86. American Mathematical Society, Providence, RI (2008)

[40] Johansson Viklund, F., Lawler, G.F.: Almost sure multifractal spectrum for the tip of an SLE curve. Acta Math. **209**(2), 265–322 (2012)

[41] Kager, W., Nienhuis, B., Kadanoff, L.P.: Exact solutions for Loewner evolutions. J. Stat. Phys. **115**(3–4), 805–822 (2004)

[42] Knizhnik, V.G., Polyakov, A.M., Zamolodchikov, A.B.: Fractal structure of 2D-quantum gravity. Mod. Phys. Lett. A **3**, 819–826 (1988)

[43] Lawler, G.F.: Conformally Invariant Processes in the Plane. Mathematical Surveys and Monographs, vol. 114. American Mathematical Society, Providence, RI (2005)

[44] Lind, J.: A sharp condition for the Loewner equation to generate slits. Ann. Acad. Sci. Fenn. **30**, 143–158 (2005)

[45] Lind, J., Marshall, D.E., Rohde, S.: Collisions and spirals of Loewner traces. Duke Math. J. **154**(3), 527–573 (2010)

[46] Loutsenko, I.: SLE$_\kappa$:correlation functions in the coefficient problem. J. Phys. A Math. Theor. **45**(27), 275001 (2012)

[47] Lawler, G.F., Werner, W.: Intersection exponents for planar Brownian motion. Ann. Probab. **27**(4), 1601–1642 (1999)

[48] Loutsenko, I., Yermolayeva, O.: Average harmonic spectrum of the whole-plane SLE. J. Stat. Mech. Theory Exp. P04007 (2013)

[49] Loutsenko, I., Yermolayeva, O.: New exact results in spectra of stochastic Loewner evolution. J. Phys. A Math. Theor. **47**(16), 165202 (2014)

[50] Loutsenko, I., Yermolayeva, O.: Stochastic Loewner evolutions, Fuchsian systems and orthogonal polynomials. J. Phys. A Math. Theor. **52**(43), 435202 (2019)

[51] Makarov, N.G.: Fine structure of harmonic measure. Rossiĭskaya Akademiya Nauk. Algebra i Analiz **10**, 1–62 (1998). (**English translation in St. Petersburg Math. J. 10: 217–268 (1999)**)

[52] Mandelbrot, B.B.: Intermittent turbulence in self-similar cascades: divergence of high moments and dimension of the carrier. J. Fluid Mech. **62**, 331–358 (1974)

[53] Marshall, D.E., Rohde, S.: The Loewner differential equation and slit mappings. J. Am. Math. Soc. **18**(4), 763–778 (2005)

[54] Painlevé, P.: Analyse des travaux scientifiques. Gauthier-Villars, Paris, 1900. Reprinted in Librairie Scientifique et Technique, Albert Blanchard, Paris, 1967, pp. 1–2; reproduced in Oeuvres de Paul Painlevé, Éditions du CNRS, Paris, 1972–1975, vol. 1, pp. 72–73

[55] Rushkin, I., Bettelheim, E., Gruzberg, I.A., Wiegmann, P.: Critical curves in conformally invariant statistical systems. J. Phys. A Math. Gen. **40**, 2165–2195 (2007)

[56] Rohde, S., Schramm, O.: Basic properties of SLE. Ann. Math. (2) **161**(2), 883–924 (2005)

[57] Rhodes, R., Vargas, V.: KPZ formula for log-infinitely divisible multifractal random measures. ESAIM Probab. Stat. **15**, 358–371 (2011)

[58] Schramm, O.: Scaling limits of loop-erased random walks and uniform spanning trees. Isr. J. Math. **118**, 221–288 (2000)

[59] Schoug, L.: A multifractal boundary spectrum for $\mathrm{SLE}_\kappa(\rho)$ curve. Probab. Theory Relat. Fields **178**, 173–233 (2020)

[60] Sheffield, S.: Conformal weldings of random surfaces: SLE and the quantum gravity zipper. Ann. Probab. **44**(5), 3474–3545 (2016)

[61] Zhan, D.: Duality of chordal SLE. Invent. Math. **174**(2), 309–353 (2008)

Bertrand Duplantier
Université Paris-Saclay
CNRS, CEA, Institut de Physique Théorique
91191 Gif-sur-Yvette Cedex
France
e-mail: `bertrand.duplantier@ipht.fr`

Yong Han
College of Mathematics and Statistics
Shenzhen University
Shenzhen 518060
Guangdong
People's Republic of China
e-mail: `hanyong@szu.edu.cn`

Chi Nguyen
Department of Information Technology
Ho Chi Minh University of Transport
2 Vo Oanh St., Ward 25, Binh Thanh District
Ho Chi Minh City
Vietnam
e-mail: `ntpchi@gmail.com`

Michel Zinsmeister
Institut Denis Poisson
Université d'Orléans
Bâtiment de mathématiques, rue de Chartres
B.P. 6759 45067 Orléans Cedex 2
France
e-mail: `zins@univ-orleans.fr`